

Synthesis of Nanoparticles and Surface Modifications

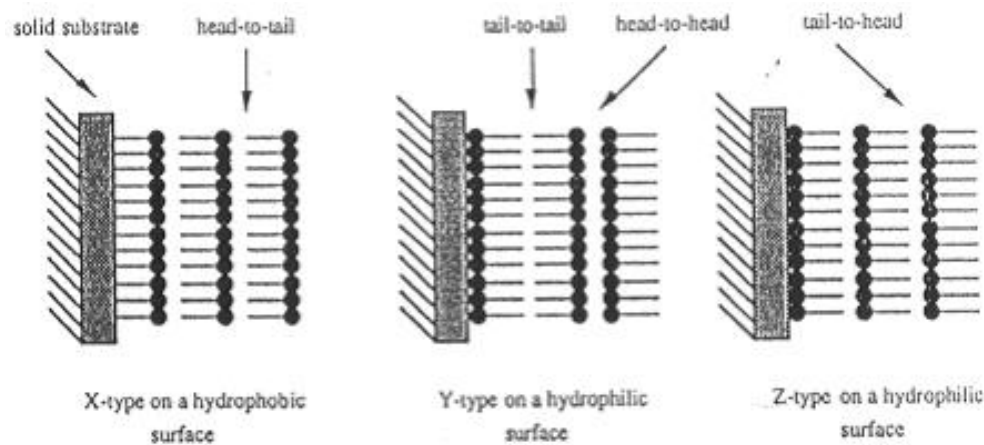
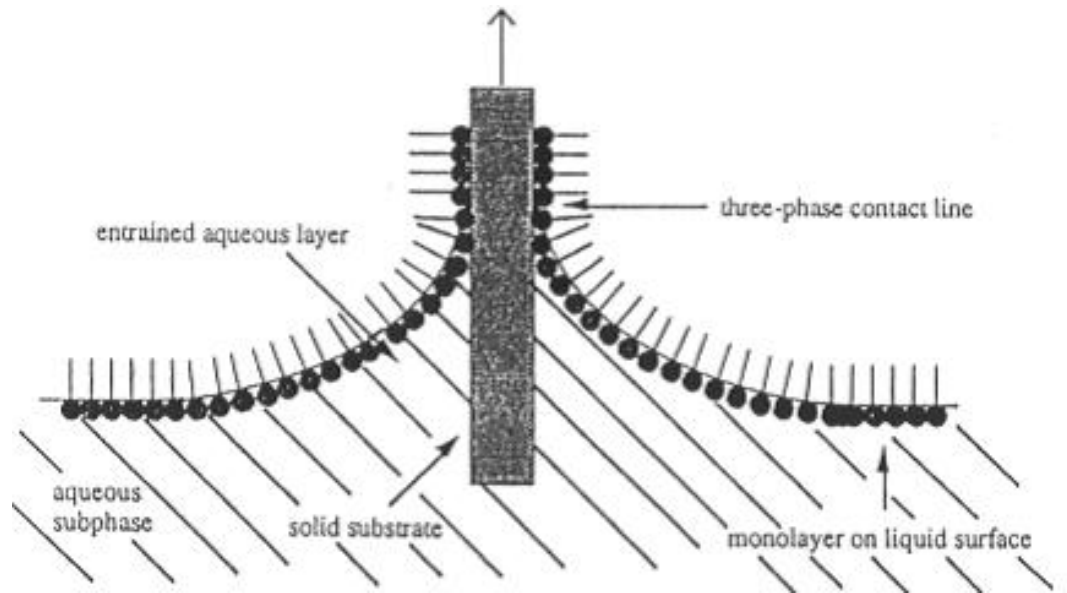
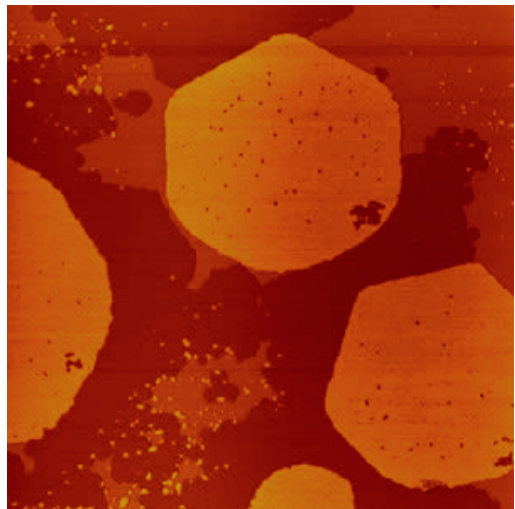


Self-Assembly

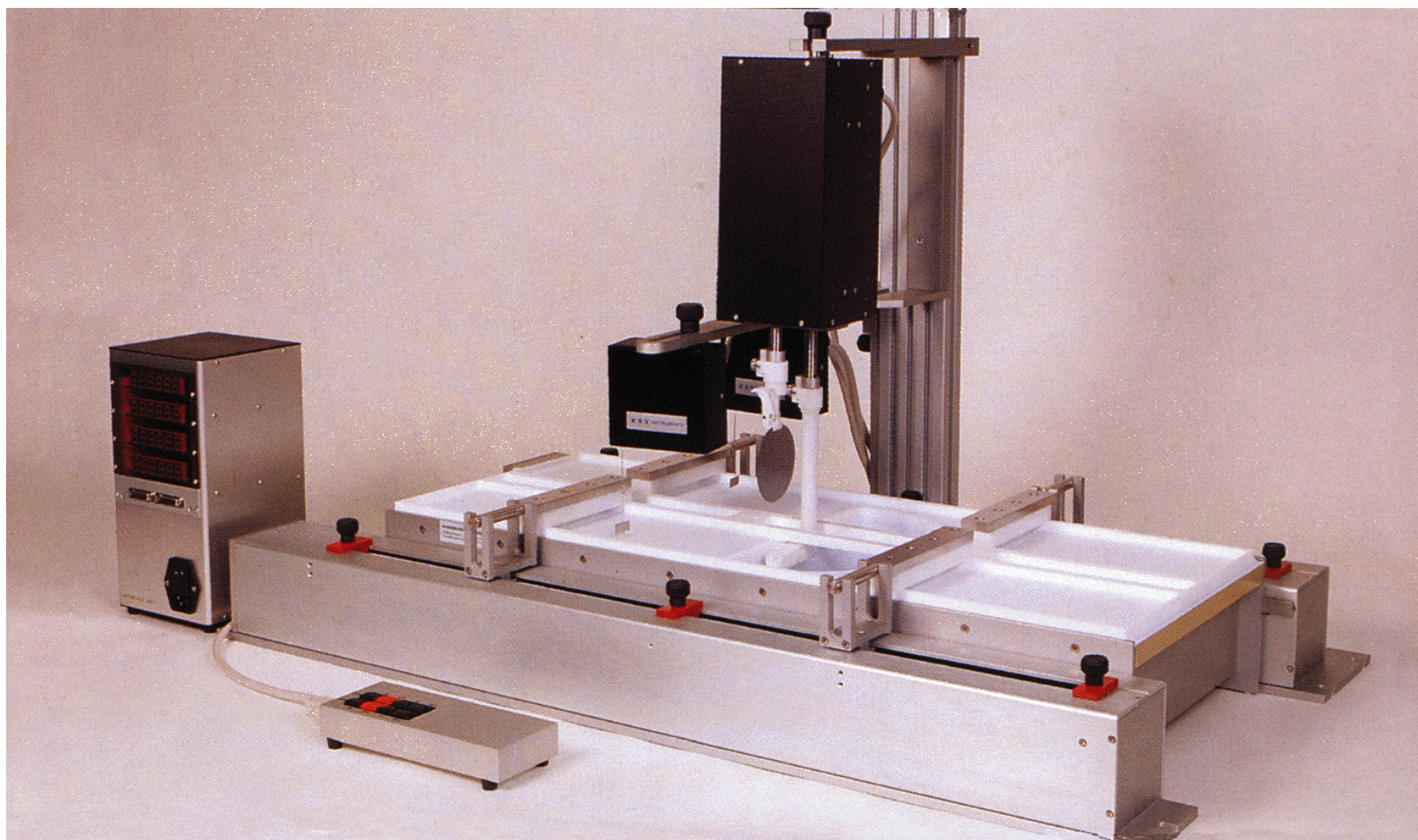
- Static assembly
- Dynamic assembly
 - $RT = 8.314 \text{ J/mol} \times 300 = 2.4 \text{ kJ/mol}$
- Driving forces
 - Chemisorption
 - Surface effect
 - Hydrophobic-hydrophilic
 - Intermolecular forces
 - Capillary force



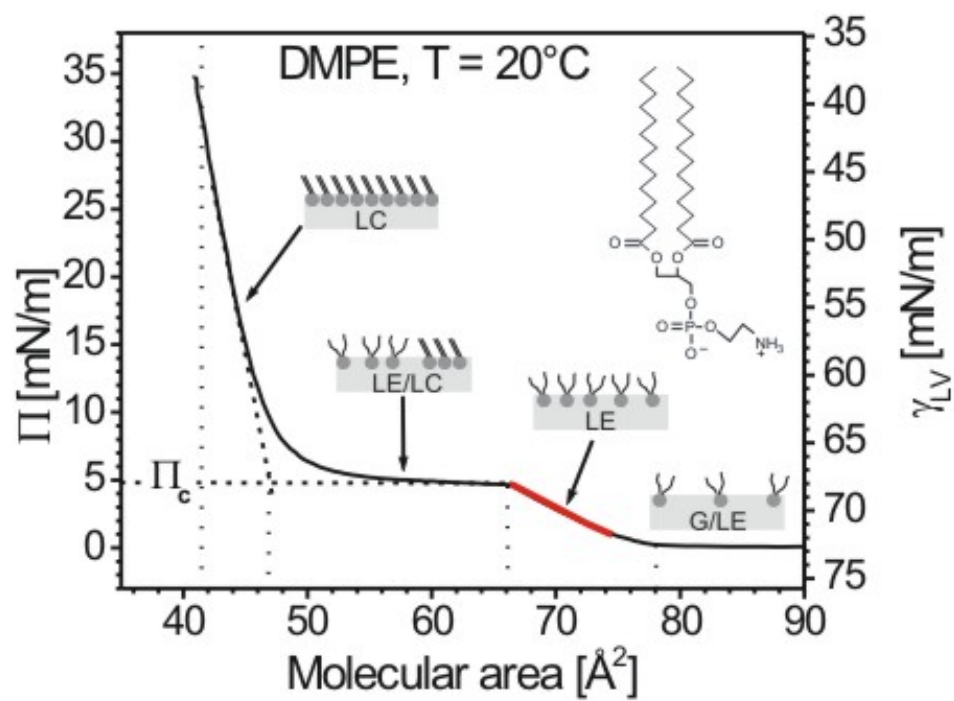
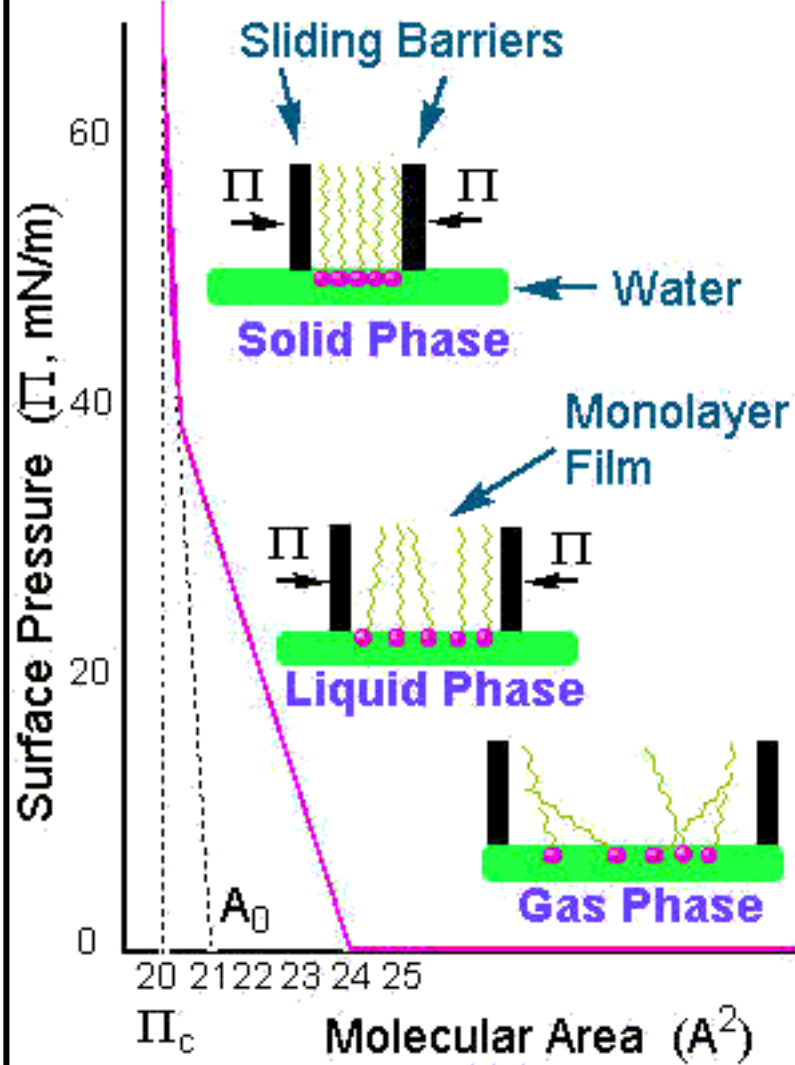
Langmuir-Blodgett Films



Langmuir-Blodgett Films



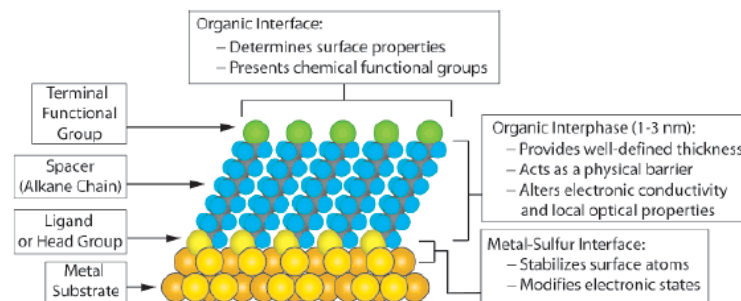
Isotherm



Self-Assemble Monolayer

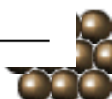
(S A M)

Chem. Rev. 2005, 105, 1103–1169



S-Au 25-30 Kcal/mole
Si-O 190 kcal/mole

Ligand	Substrates	Morphology of Substrate		Ligand	Substrates	Morphology of Substrate	
		Thin Films or Bulk Material	Nanoparticles or Other Nanostructures			Thin Films or Bulk Material	Nanoparticles or Other Nanostructures
ROH	Fe ₃ O ₄ Si-H Si	36 37	35	RSSR'	Ag Au CdS Pd Au	89 20 30 93	90 90-92 61
RCOO-/RCOOH	α-Al ₂ O ₃ Fe ₃ O ₄ Ni Ti/TiO ₂	38,39	40 41,42				
RCOO-OOCR	Si(111):H Si(100):H	44					
Ene-diol	Fe ₃ O ₄	45					
RNH ₂	FeS ₂ Mica Stainless Steel 316L YBa ₂ Cu ₃ O _{7-δ}	46 47 48 49			RS ₂ O ₃ ²⁻ Na ⁺ Au CdSe	94 96 97	95
	CdSe	50			RSeH	Ag Au CdS CdSe	99 100,101 60 102
RC≡N	Ag Au	51			RSeSeR'	Au	101
R-N≡N ⁺ (BF ₄ ⁻)	GaAs(100) Pd Si(111):H	52 52 52			R ₃ P	Au FeS ₂ CdS CdSe CdTe	103 104 104 104
RSH	Ag Ag ₉₀ Ni ₁₀ AgS Au AuAg AuCu Au _x Pd _{1-x} CdTe CdSe CdS Cu FePt GaAs Ge Hg HgTe InP Ir Ni PbS Pd PdAg Pt Ru Stainless Steel 316L YBa ₂ Cu ₃ O _{7-δ} Zn ZnSe ZnS	26 55 56 26 57 58 58 58 59 60 61,62 26 58 63-66 67 68 69-71 72 73 74 75 76-78 30 74,79 58 32 80 81 48 82 83 84 85 86 87 88	53,54 55 56 57 58 58 58 58 59 60 61,62 58 58 63-66 67 68 69-71 72 73 74 75 76-78 74,79 58 80 81 76-78 74,79 80 81 82 83 84 85 86 87 88		R ₃ P=O	Co CdS CdSe CdTe	105,106 104 104 104
					RPO ₃ ²⁻ /RP(O)(OH) ₂	Al Al-OH Ca ₁₀ (PO ₄ ,CO ₃) ₆ (OH) ₂ GaAs GaN Indium tin oxide (ITO) Mica TiO ₂ ZrO ₂ CdSe CdTe	107 108 109 110 110 111 112 113,114 114,115 116-118 118,119
					RPO ₄ ³⁻	Al ₂ O ₃ Nb ₂ O ₅ Ta ₂ O ₅ TiO ₂	120 120 121 120,122
					RN≡C RHC-CH ₂ RC≡CH	Pt Si Si(111):H	123 37 125
RSAc	Au Au	86 87			RSiX ₃	HfO ₂	126
RSR'	Au	88				ITO PtO TiO ₂ ZrO ₂	127 128 113,126,129 126,129



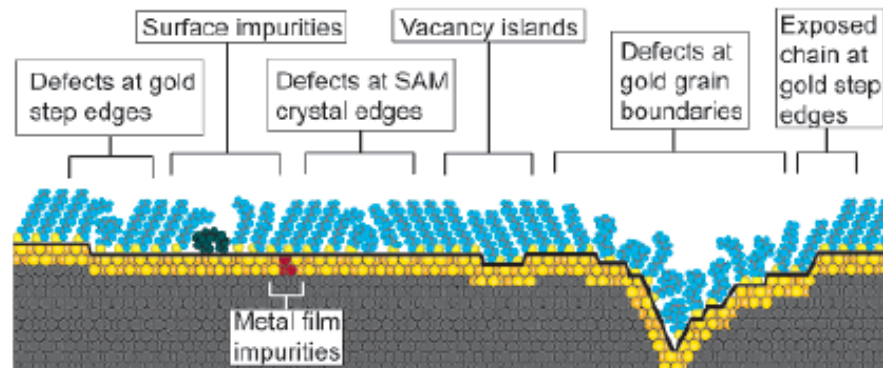
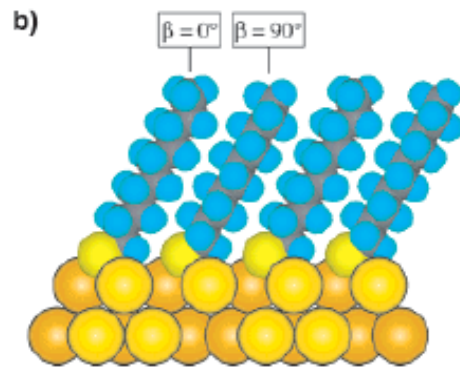
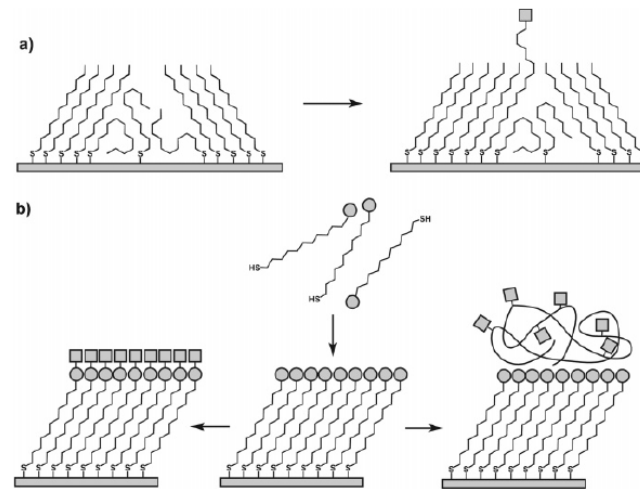
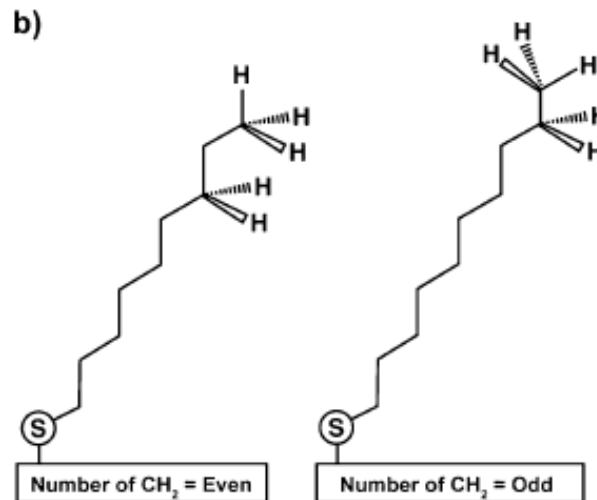


Figure 7. Schematic illustration of some of the intrinsic and extrinsic defects found in SAMs formed on polycrystalline substrates. The dark line at the metal–sulfur interface is a visual guide for the reader and indicates the changing topography of the substrate itself.



^a (a) Insertion of a functional adsorbate at a defect site in a preformed SAM. (b) Transformation of a SAM with exposed functional groups (circles) by either chemical reaction or adsorption of another material.



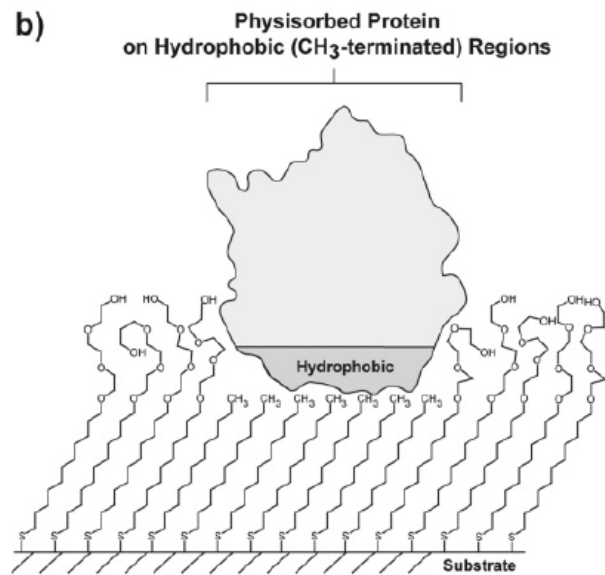
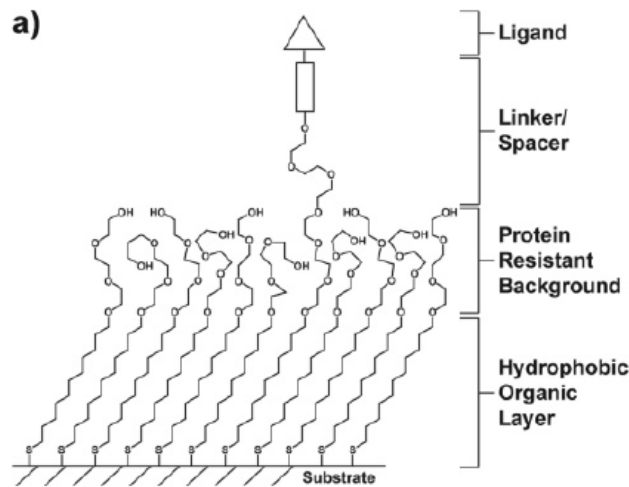


Figure 21. Schematic illustrations of (a) a mixed SAM and (b) a patterned SAM. Both types are used for applications in biology and biochemistry.

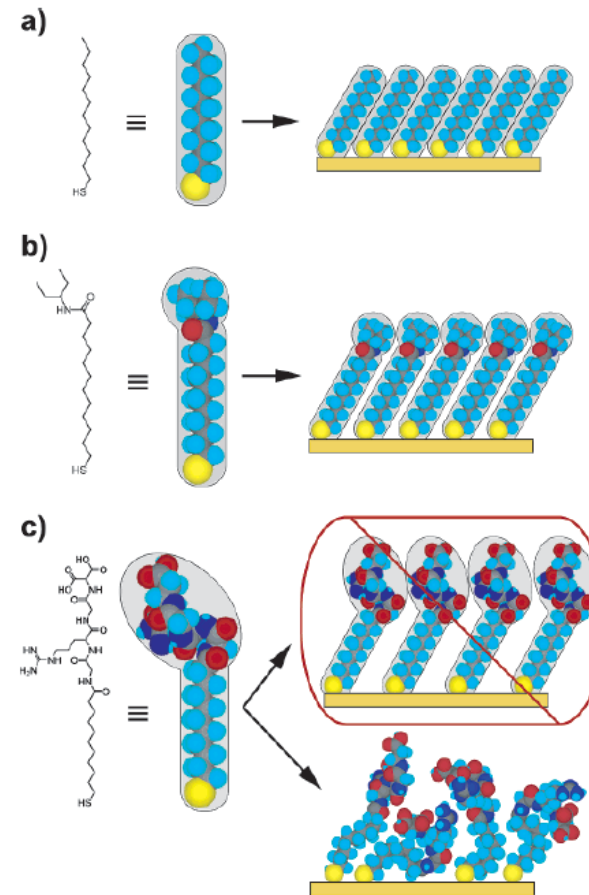


Figure 22. Schematic diagram illustrating the effects that large terminal groups have on the packing density and organization of SAMs. (a) Small terminal groups such as $-\text{CH}_3$, $-\text{CN}$, etc., do not distort the secondary organization of the organic layer and have no effect on the sulfur arrangement. (b) Slightly larger groups (like the branched amide shown here) begin to distort the organization of the organic layer, but the strongly favorable energetics of metal–sulfur binding drive a highly dense arrangement of adsorbates. (c) Large terminal groups (peptides, proteins, antibodies) sterically are unable to adopt a secondary organization similar to that for alkanethiols with small terminal groups. The resulting structures probably are more disordered and less dense than those formed with the types of molecules in a and b.



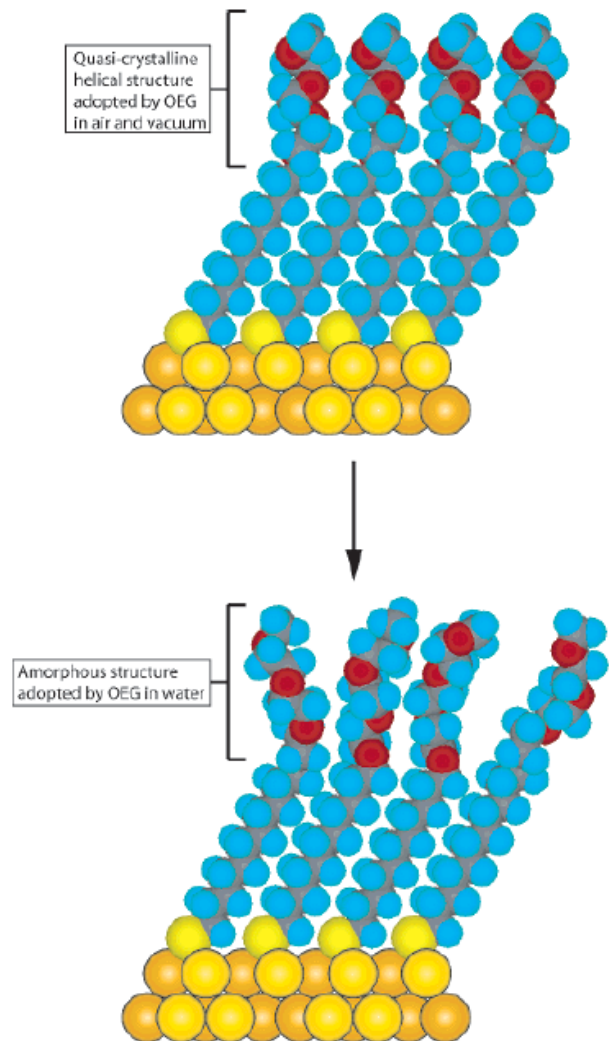
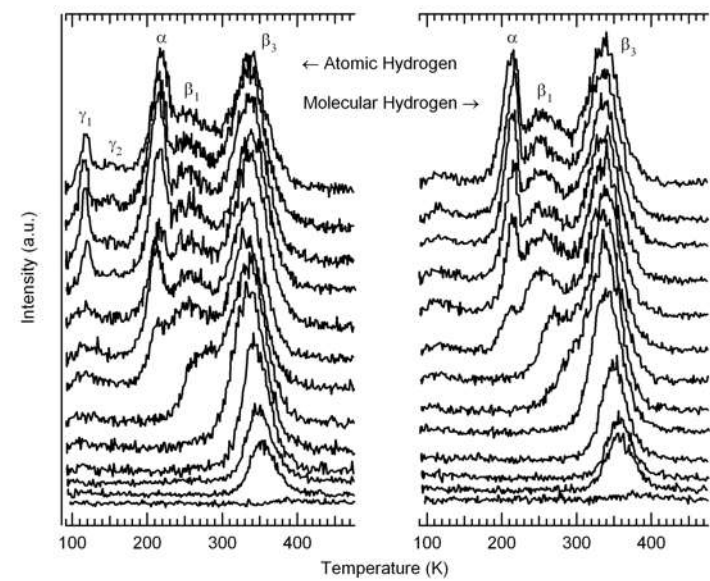
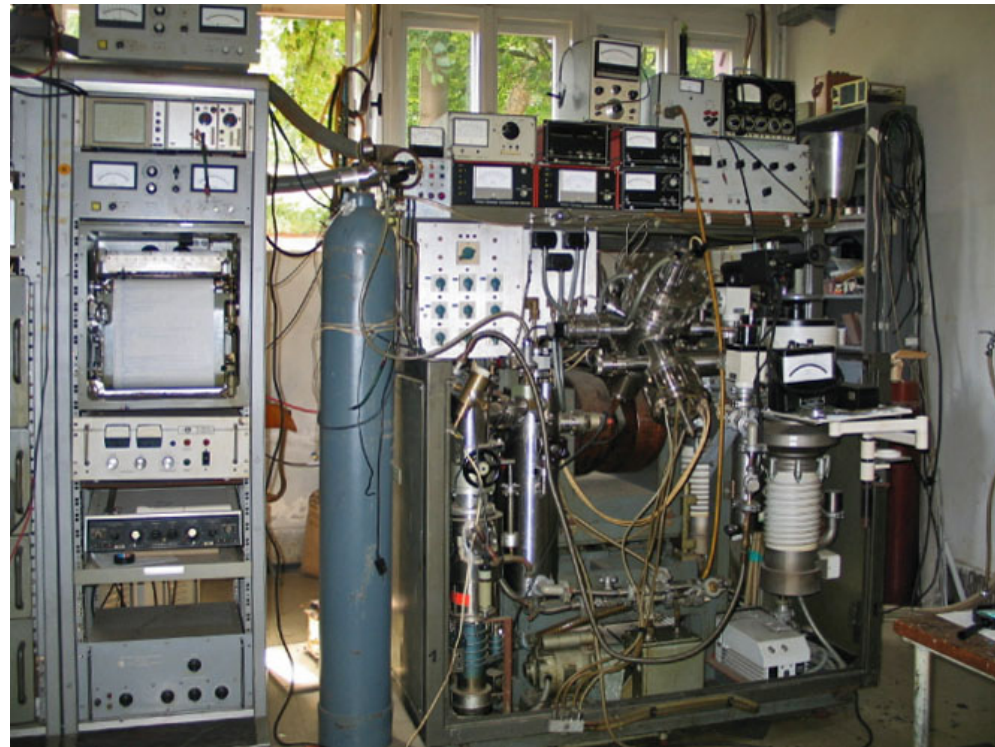


Figure 23. Schematic illustration of the order–disorder transition evidenced by SAMs of alkanethiolates terminated with triethylene glycol. The EG₃ group loses conformational ordering upon solvation in water.



Temperature Programmed Desorption



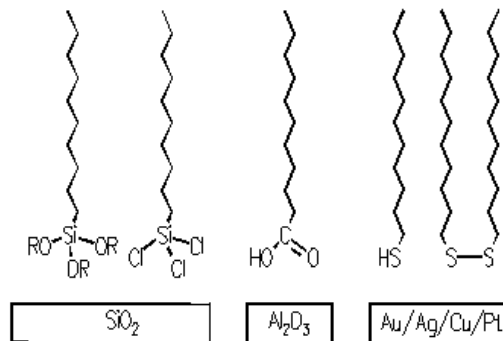
Self-Assembly

- Substrates
- Interstitial adhesion layer
- Noble metal layer
- Organo-sulfur



Organosilanes

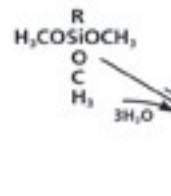
Self-assembled monolayers



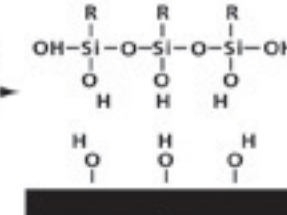
- Surface
- silicon oxide: silanisation
- aluminum oxide: fatty acids
- metals: thiols and sulfides

Immersion of substrate in a solution containing the adequate molecules for 12 - 24 hours yields an ordered monolayer

Hydrolysis (1)



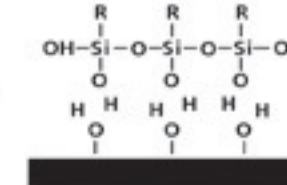
Condensation of Oligomers (2)



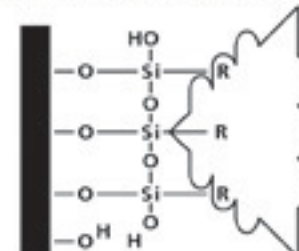
Bond Formation (4)



Hydrogen Bonding (3)

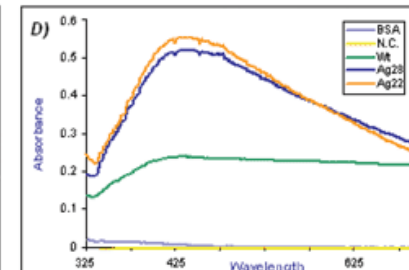
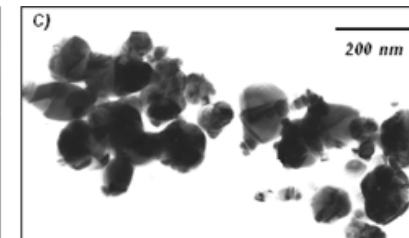
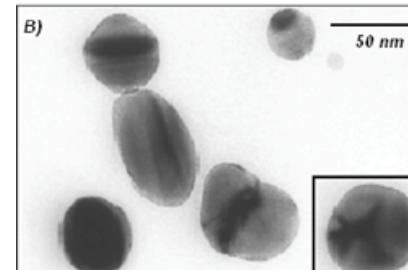
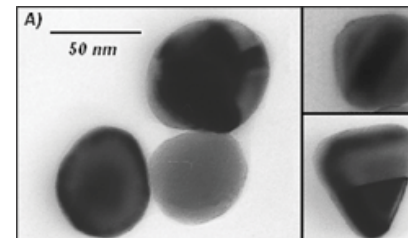
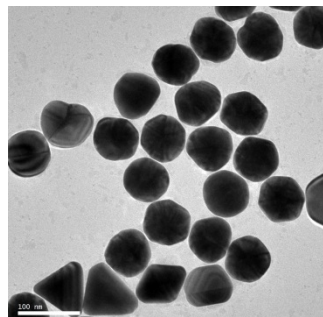
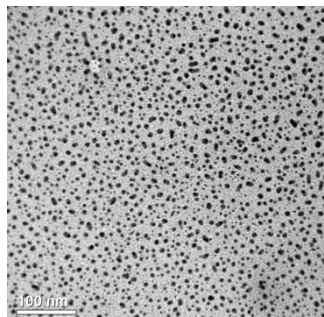
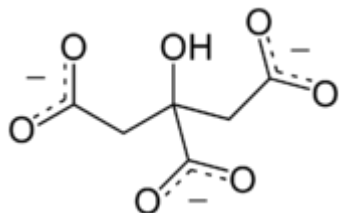


Reaction and bond formation of the R group (5)



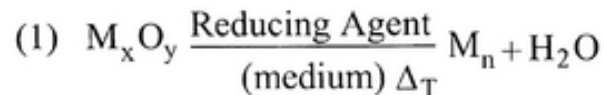
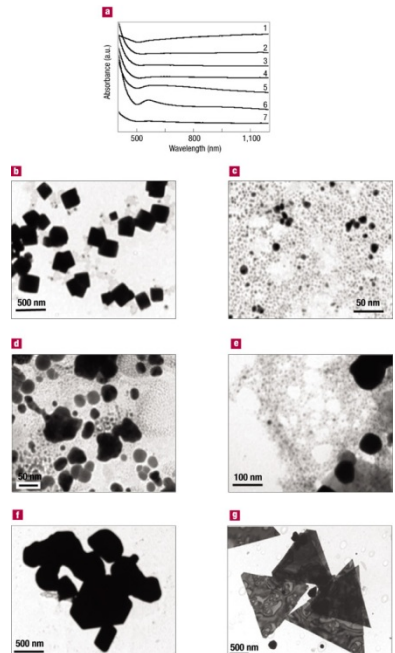
Synthesis of Silver Nanoparticles

1. A solution of AgNO_3 ($1.0 \times 10^{-3} \text{ M}$) in deionized water was heated until it began to boil.
2. Sodium citrate solution was added dropwise to the silver nitrate solution as soon as the boiling commenced. The color of the solution slowly turned into grayish yellow, indicating the reduction of the Ag^+ ions.
3. Heating was continued for an additional 15 min, and then the solution was cooled to room temperature before employing for further experimentation.

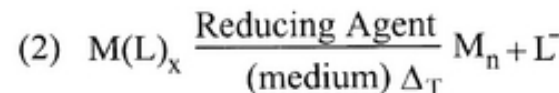


Synthesis of Gold Nanoparticles

1. Add 20 mL of 1.0 mM HAuCl_4 to a 50 mL round bottom flask on a stirring hot plate.
2. Add a magnetic stir bar and bring the solution to a boil.
3. To the boiling solution, add 2 mL of a 1% solution of trisodium citrate dihydrate
4. The gold sol gradually forms as the citrate reduces the gold(III). Stop heating when a deep red color is obtained.



(Reducing Agent = $\text{R} - \text{COH}$)



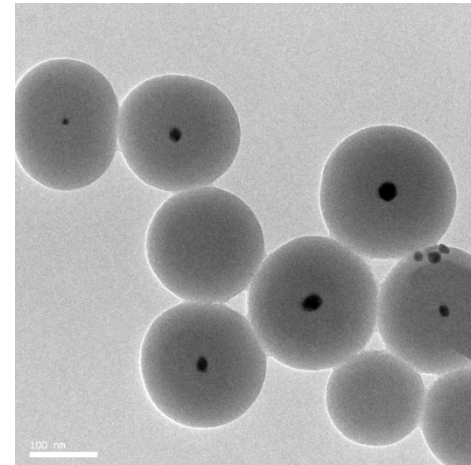
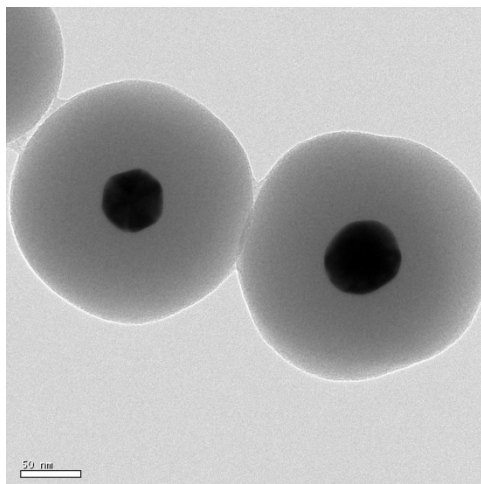
($\text{L} = \text{NO}_3^-, \text{C}_2\text{H}_5\text{O}^-$)

(Reducing Agent = $\text{R} - \text{COH}$)

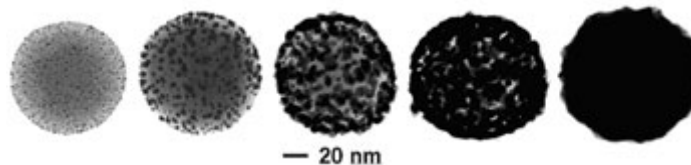
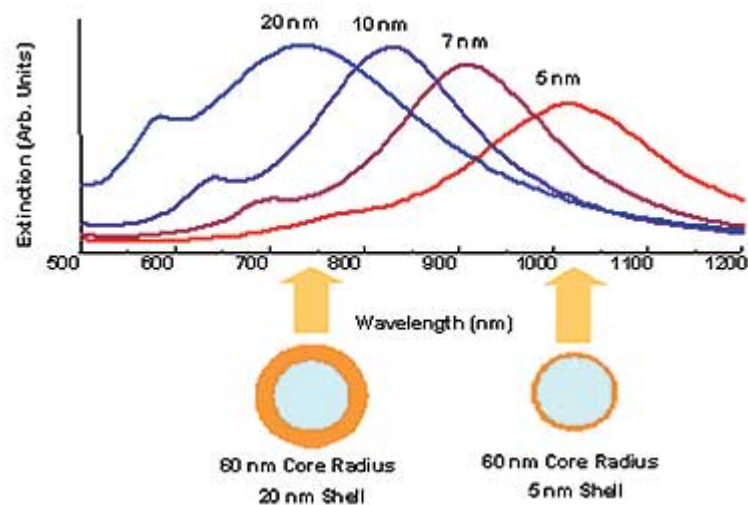


Construction of Core Shell Ag/Au@SiO₂ Nanoparticles

1. Under vigorous stirring, 1 ml of the silver/ gold colloids solution was mixed with 250 mL of isopropanol and 25 mL of deionized water.
2. Immediately after the addition of 4 mL of 30% ammonium hydroxide, different amounts of tetraethoxysilane (TEOS) were added to the reaction mixture.
3. To obtain different silica layer thicknesses, TEOS solutions with a concentration between 50% and 100% was added to the suspension. The reaction was stirred at room temperature for 30 minutes and then was allowed to age without agitation at 4°C overnight.
4. Each suspension of silica-coated silver/gold nanoparticles was washed and centrifuged, followed by re-suspension in water. The thickness of the silica layers was determined from TEM images .



Core-Shell Nanoparticles



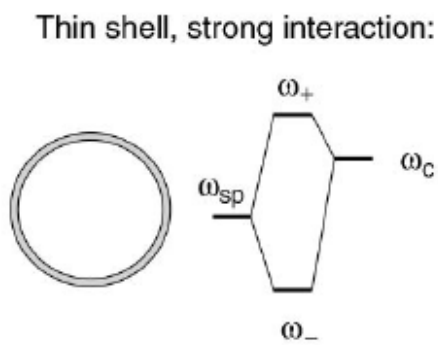
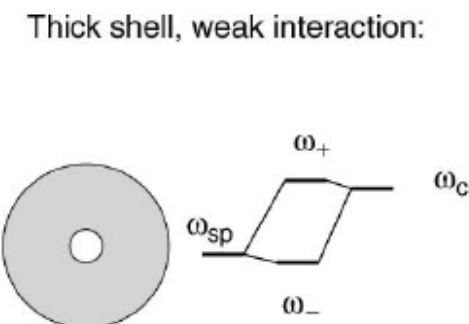
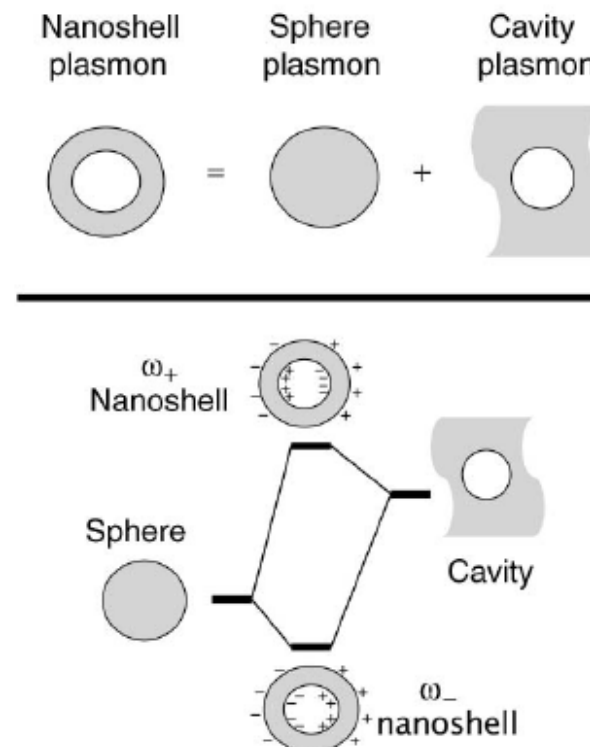
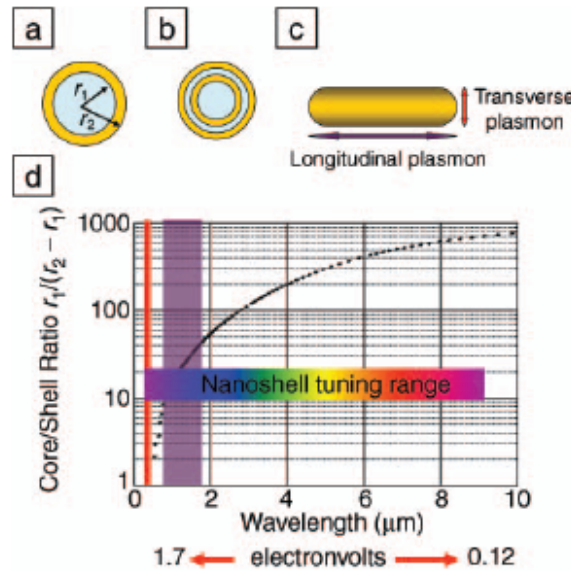


Figure 2. Plasmon hybridization and the sphere–cavity model for nanoshells: the interaction between a sphere (resonance frequency, ω_{sp}) and a cavity plasmon (resonance frequency, ω_c) is tuned by varying the thickness of the shell layer of the nanoparticle. Two hybrid plasmon resonances, the ω_- “bright,” or “bonding,” plasmon and the ω_+ “dark,” or “anti-bonding,” plasmon resonances are formed. The lower-energy plasmon couples most strongly to the optical field.



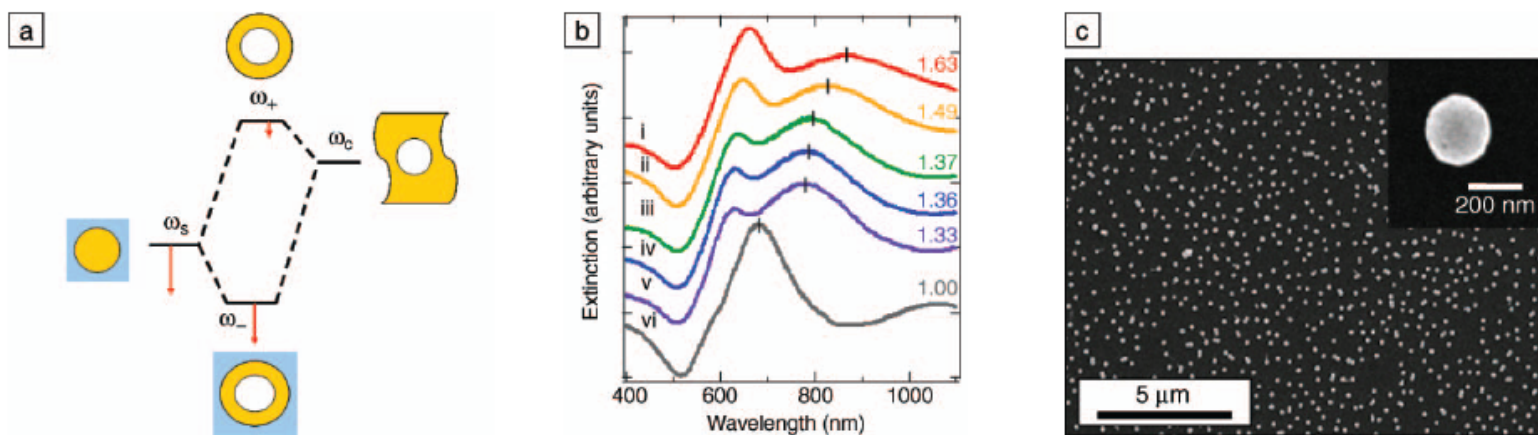


Figure 5. (a) Plasmon hybridization picture applied to surface plasmon resonance sensing with nanoshells: the low-energy “bonding” plasmon, ω_- , is sensitized to changes in its dielectric environment. The blue background schematically denotes the embedding medium for the nanoparticle. (b) Experimental curves showing plasmon resonance shifts for nanoshell-coated films in various media: (i) carbon disulfide, (ii) toluene, (iii) hexane, (iv) ethanol, (v) H_2O , and (vi) air. The index of refraction for each embedding medium is noted on the far right of the spectra. Spectra are offset for clarity. (c) Scanning electron micrograph of nanoshells deposited onto a poly(vinyl pyridine) functionalized glass surface, as used to acquire data in (b). Inset: individual nanoshell.



Preparation of $\text{Fe}_3\text{O}_4@\text{Ag}/\text{Au}$

1. *To the magnetic nanoparticle suspension obtained from commercial company, add 50 ml of a solution of Au (III) salt or Ag (I) salt at concentration of 0.01–1% mmol/L, shaking for 30 minutes, allowing Au (III) or Ag (I) ion to absorb on the surface of magnetic nanoparticle sufficiently,*
2. *Then adding 15–40 ml of reducing agent, such as hydroxylamine hydrochloride at concentration of 40 mmol/L, reacting for 5–40 minutes.*
3. *Further adding 1–10 ml of a solution of Au (III) salt or Ag (I) salt at concentration of 0.01–1%, shaking for 10 minutes, coating a reduced layer of gold or silver on the surface of the magnetic nanoparticle, forming super-paramagnetic composite particles having core/shell structure, separating magnetically, washing repeatedly with distilled water.*



Synthesis of Quantum Dots

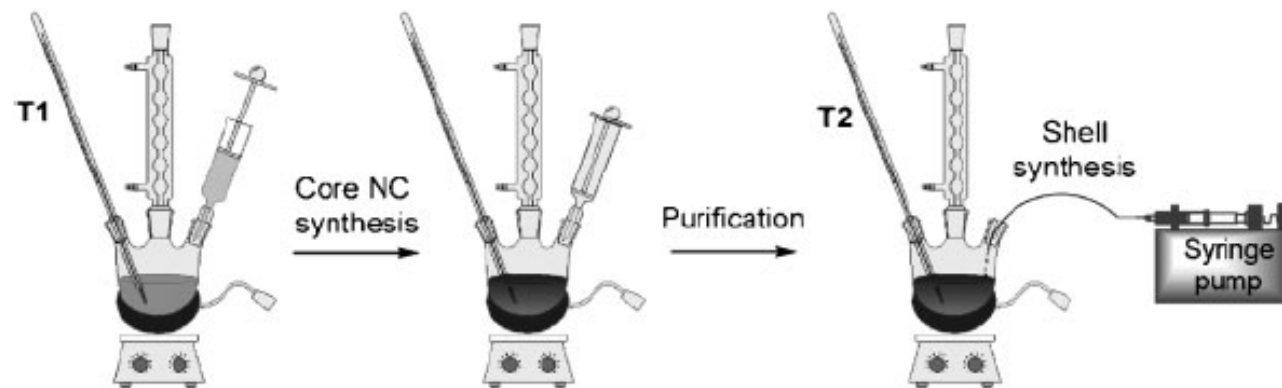
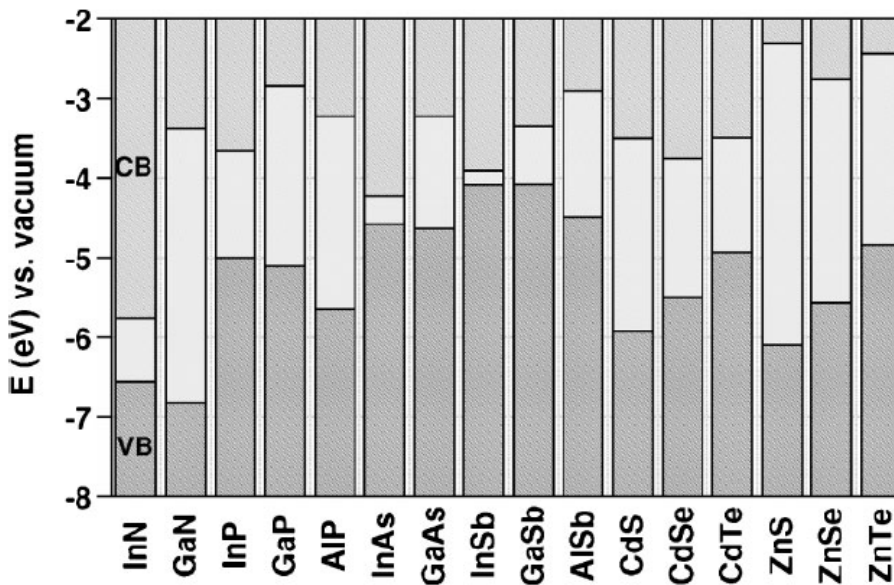


Figure 2. Two-step synthesis of core/shell nanocrystals.





Scheme 1. Electronic energy levels of selected III-V and II-VI semiconductors using the valence-band offsets from Reference [12] (VB: valence band, CB: conduction band).

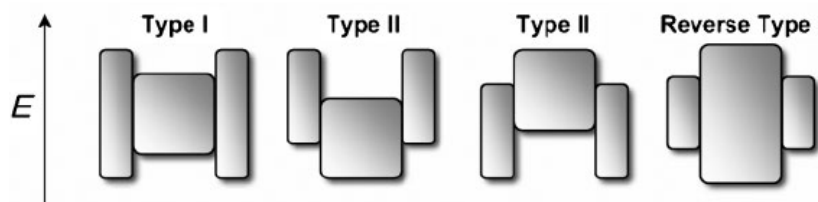
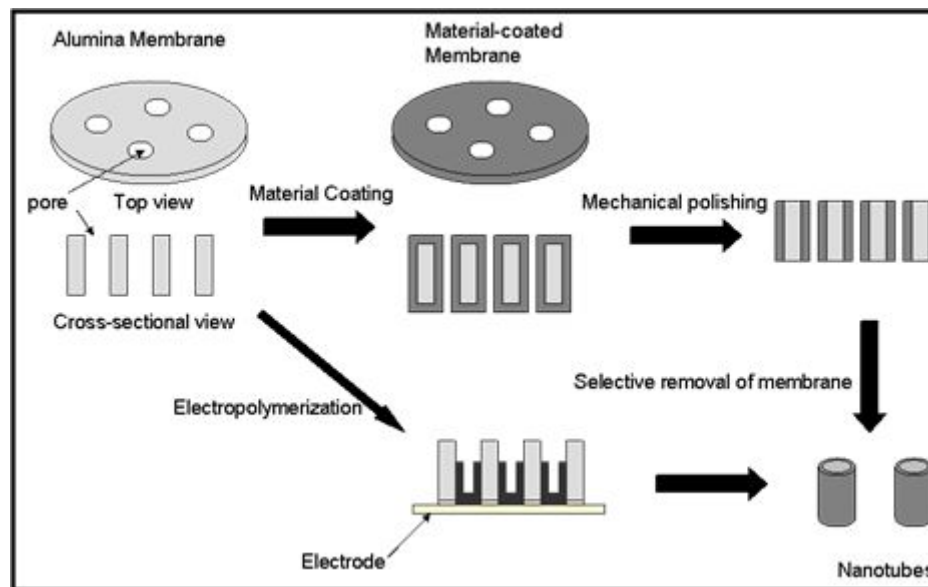


Figure 1. Schematic representation of the energy-level alignment in different core/shell systems realized with semiconductor NCs to date. The upper and lower edges of the rectangles correspond to the positions of the conduction- and valence-band edge of the core (center) and shell materials, respectively.



Template Synthesis



Porous Materials

- AAO
- MCM-41

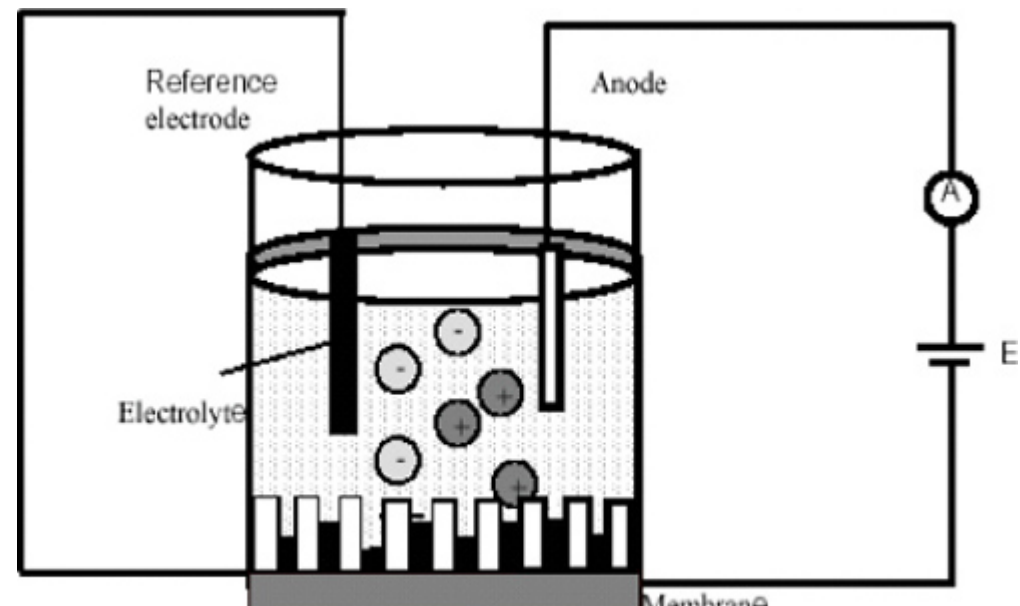
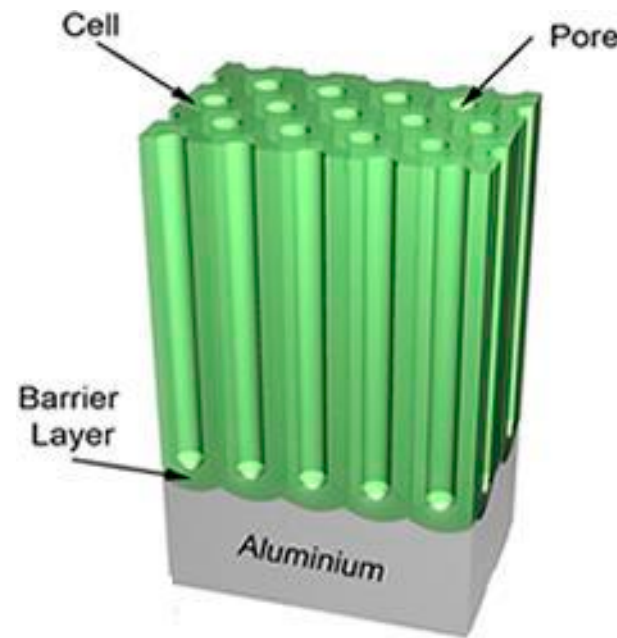
Mobil Crystalline Materials, or MCM-41

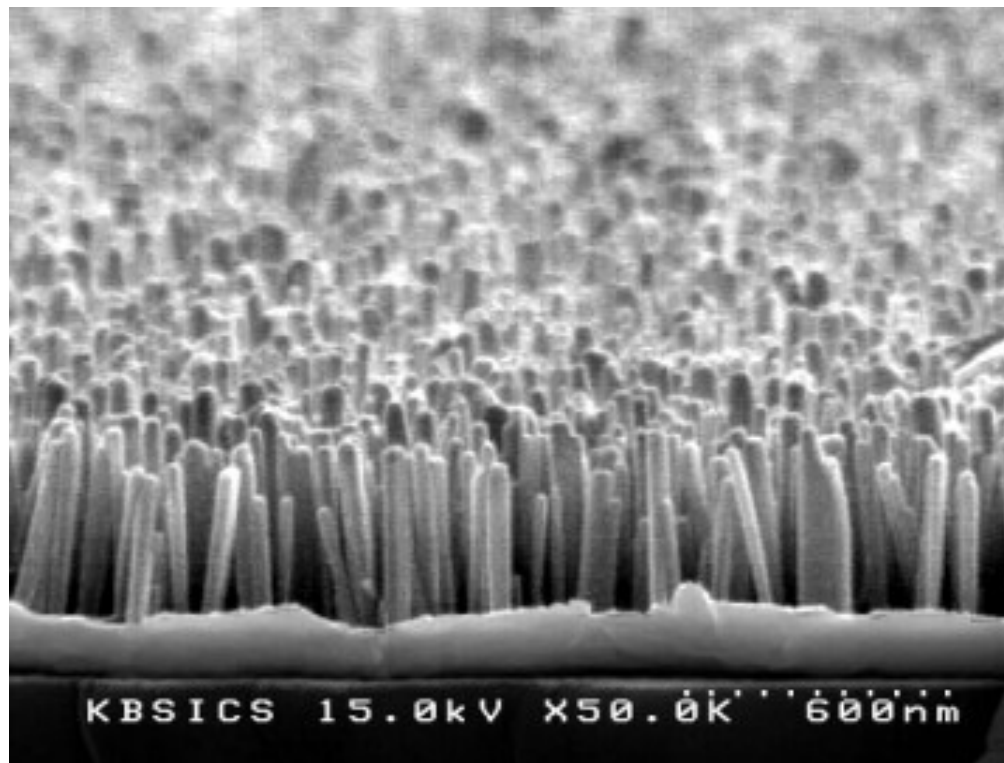
Santa Barbara Amorphous type material, or SBA-15

- Micro: $< 2\text{nm}$
- Meso:
- Macro: $> 50\text{nm}$



AAO





KBSI CS 15.0kV X50.0K 600nm



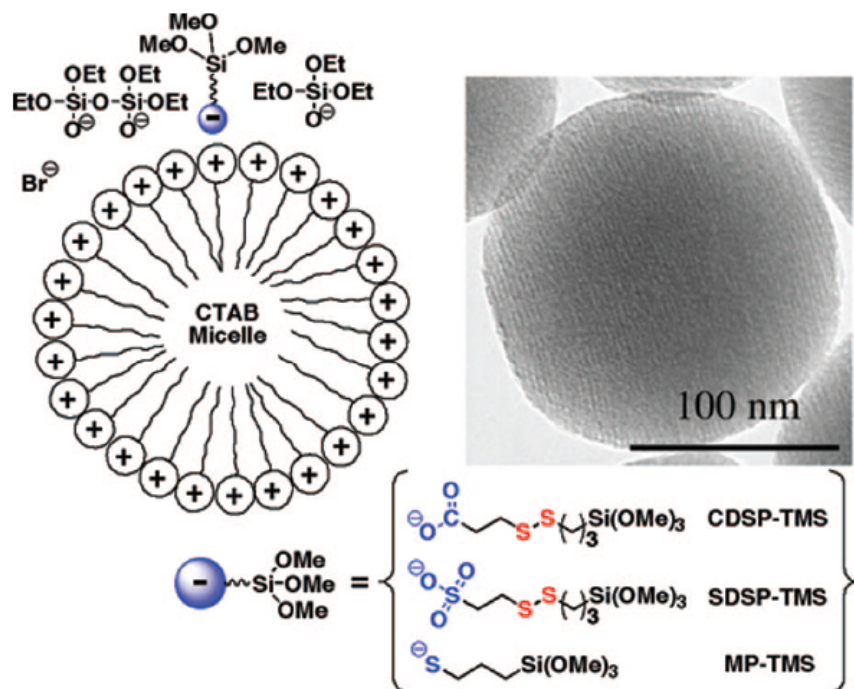


FIGURE 3. Schematic representation of the use of anionic organoalkoxysilanes for controlling the functionalization of the MSN materials. The MCM-41-type mesoporous channels are illustrated by the parallel stripes shown in the transmission electron microscopy (TEM) micrograph of the MSN-SH material. Reproduced with permission from ref 15. Copyright 2005, Royal Society of Chemistry.



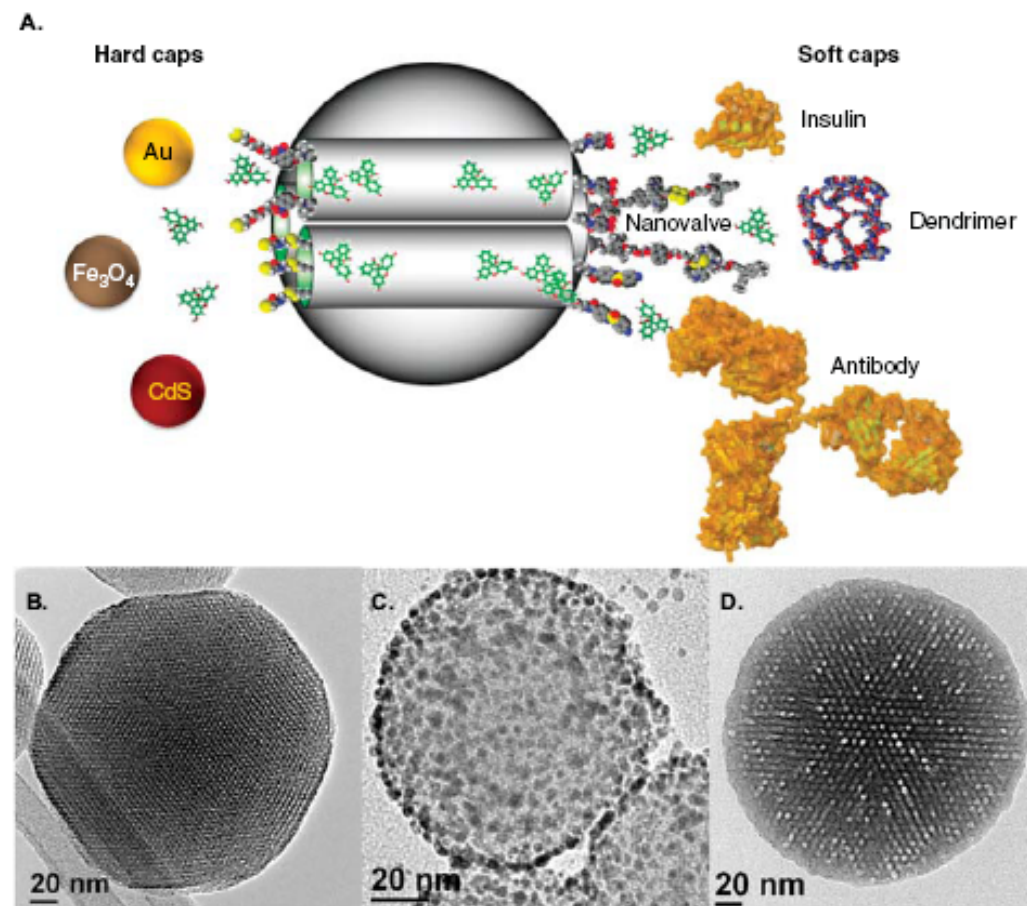


Figure 1. A. Schematic representation of a MSN loaded with drugs and capped with hard caps and soft caps highlighted in this review. Transmission electron microscopy images of (B) a MSN along the axis of the mesopores, (C) capped with hard (Au NP) and (D) with soft (polymer) caps.

MSN: Mesoporous silica nanoparticle.



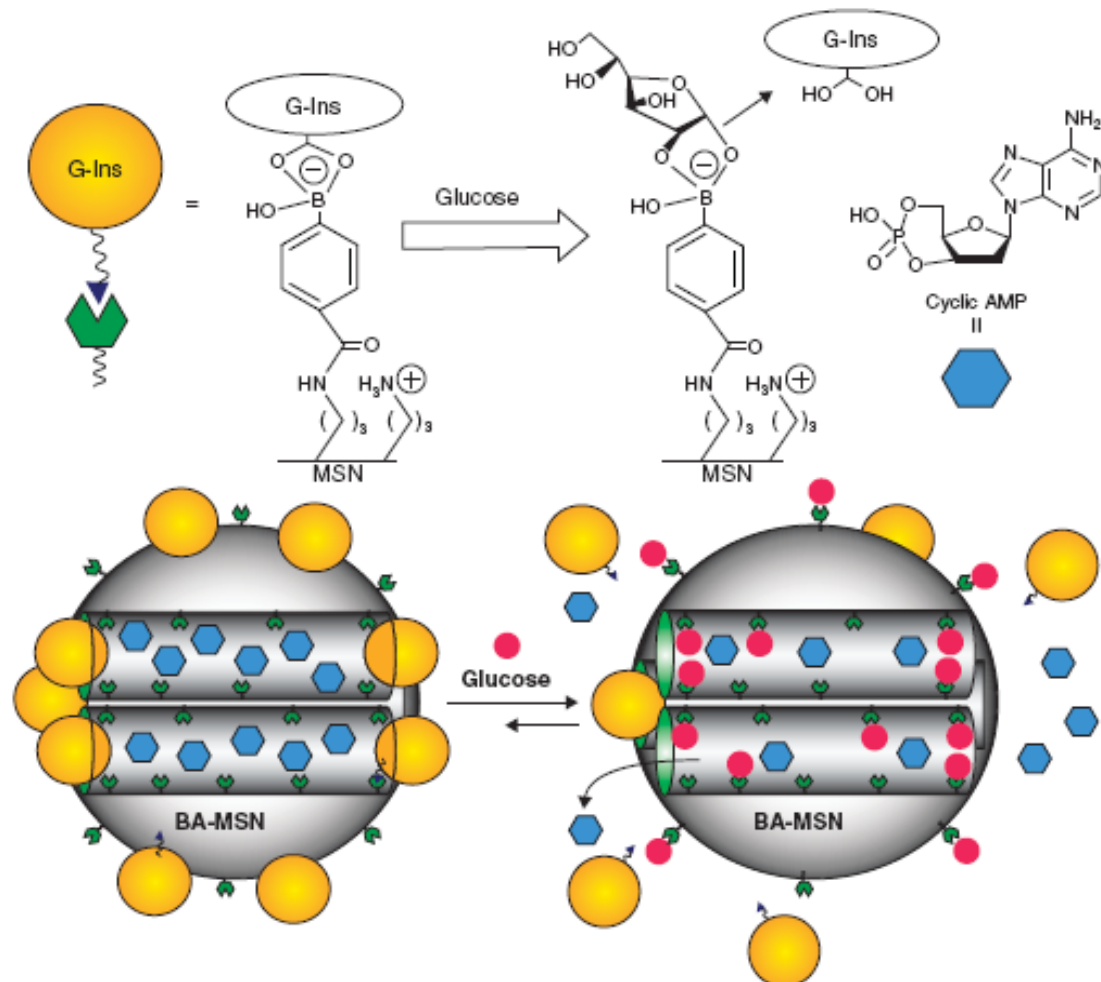


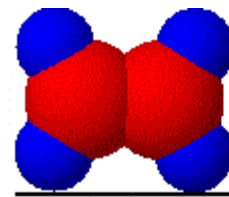
Figure 5. Schematic representation of the glucose-responsive MSN-based double delivery system for controlled release of bioactive G-Ins and cyclic AMP. The controlled release mechanism was achieved by means of the displacement reaction between blood glucose and G-Ins based on reversible boronic acid-diol complexation. High glucose concentration triggers the G-Ins uncapping and the release of cyclic AMP sequentially to diminish the higher than normal level of blood glucose.

Reproduced with permission from [19].

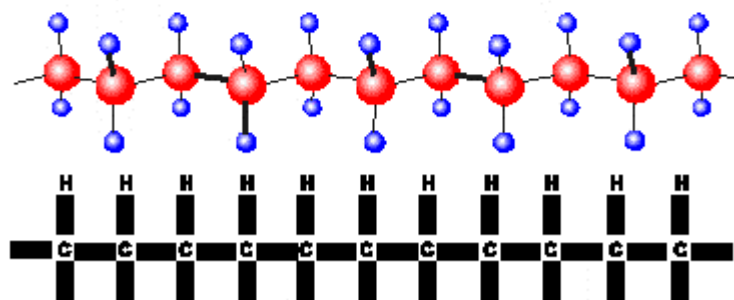
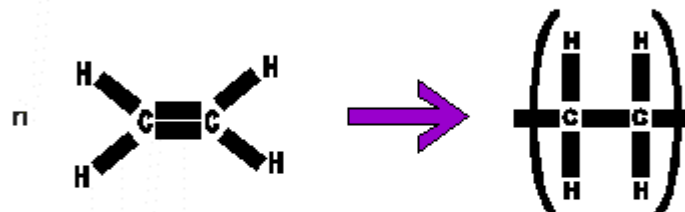
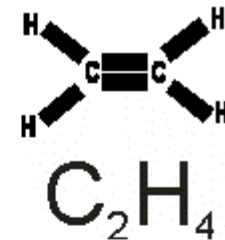
G-Ins: G-insulin; MSN: Mesoporous silica nanoparticle.



Polymer



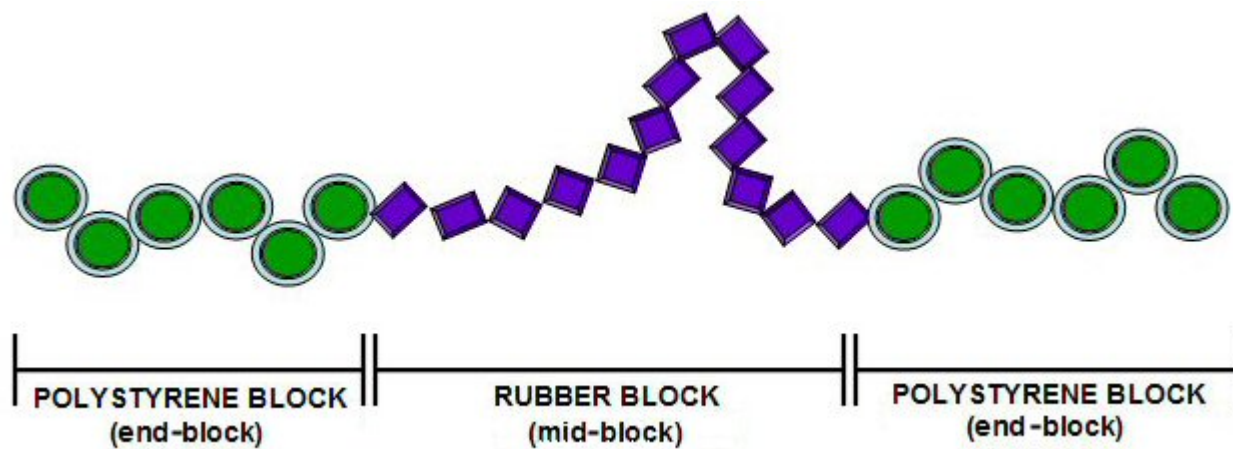
a monomer ethene



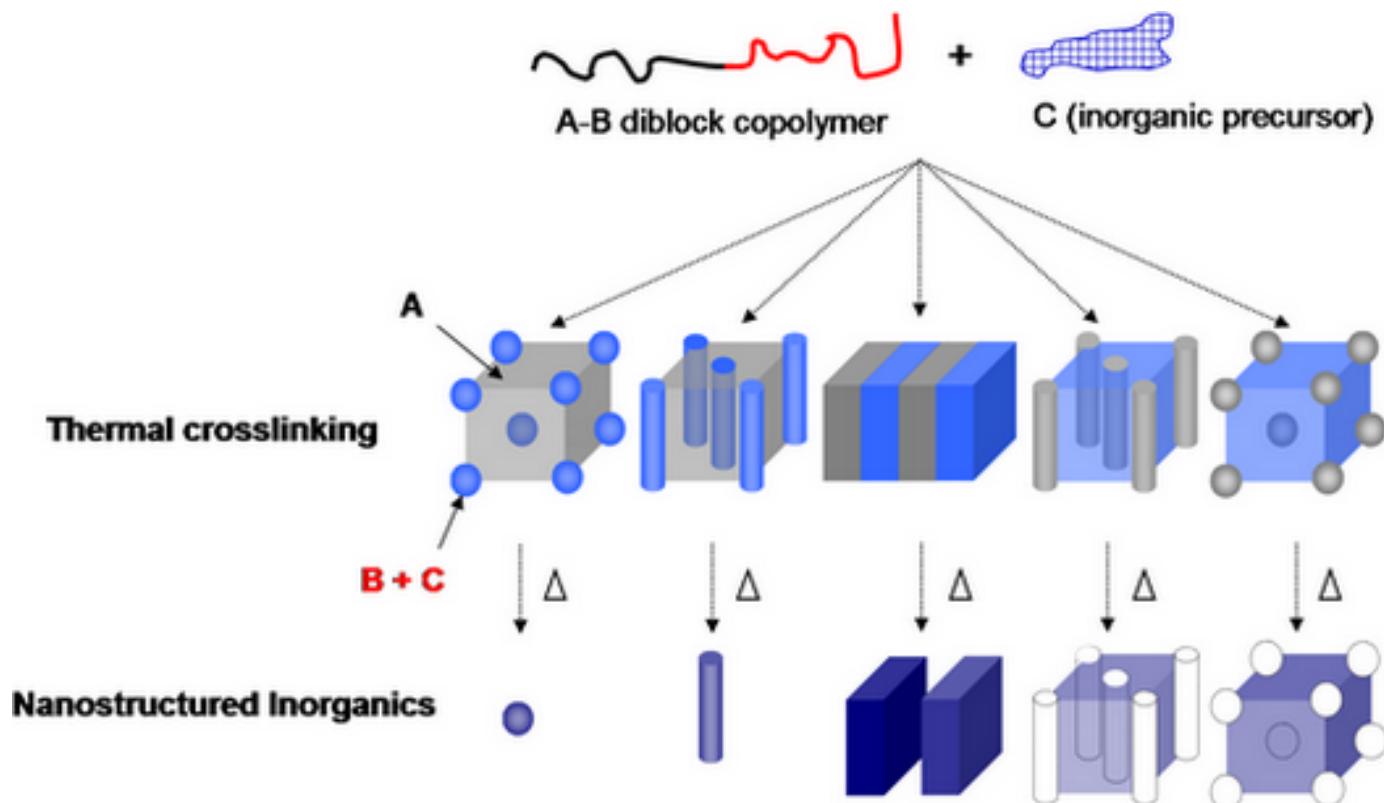
a polymer poly(ethene)



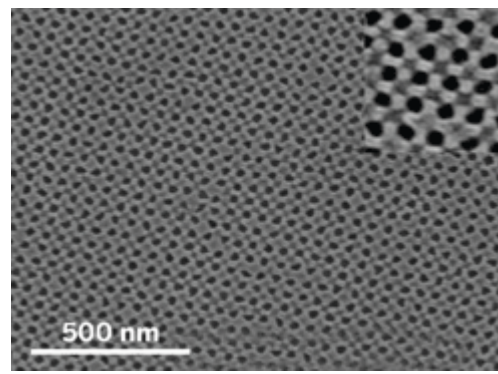
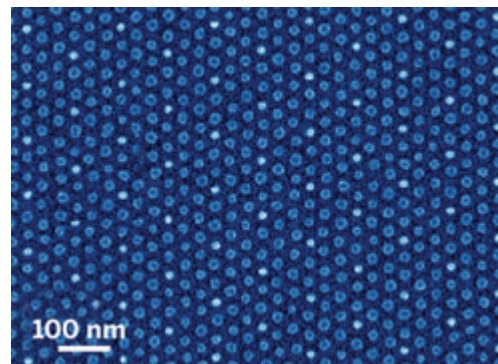
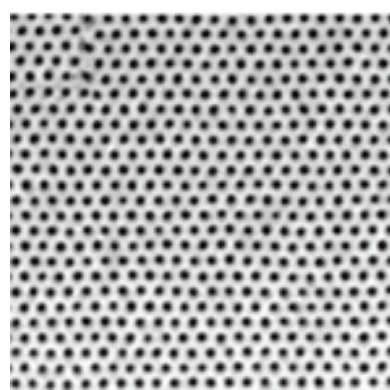
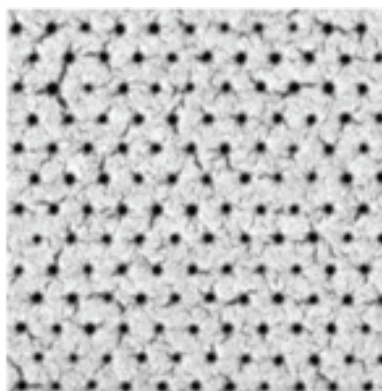
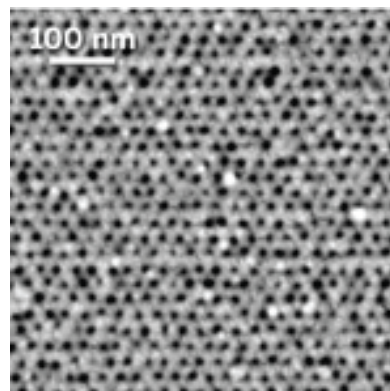
Block copolymer



Phase Segregation



Self-Assembled Block-copolymer



CNT

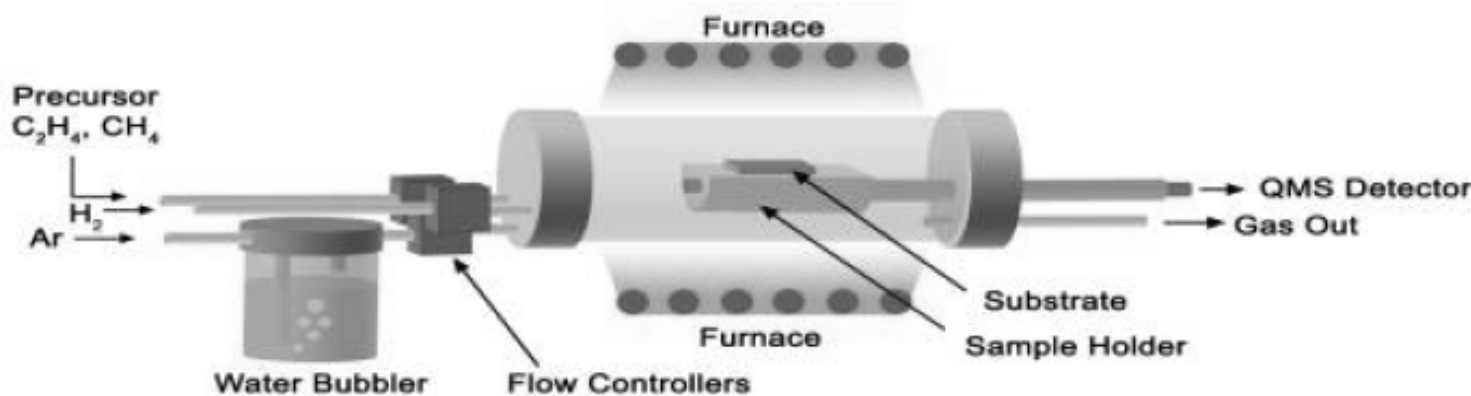
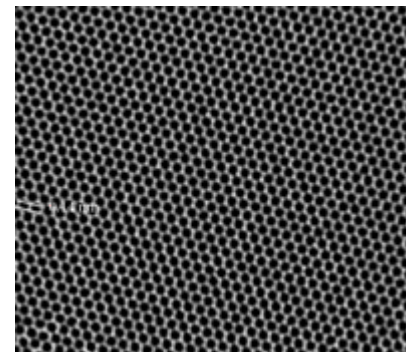
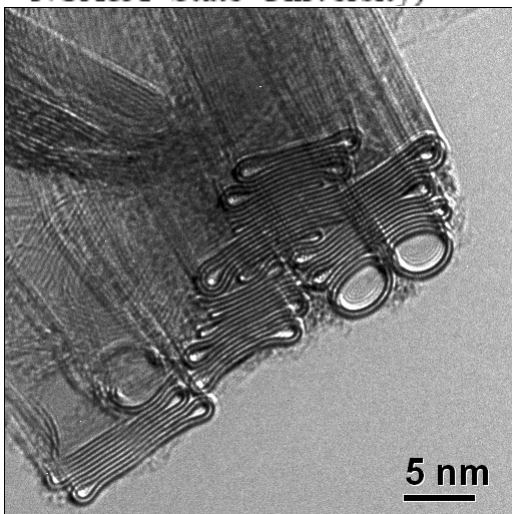


Fig. 1. Schematic of a CVD reactor for carbon nanotube growth. (Sketch by S. Yarmolenko from NCA&T State University)

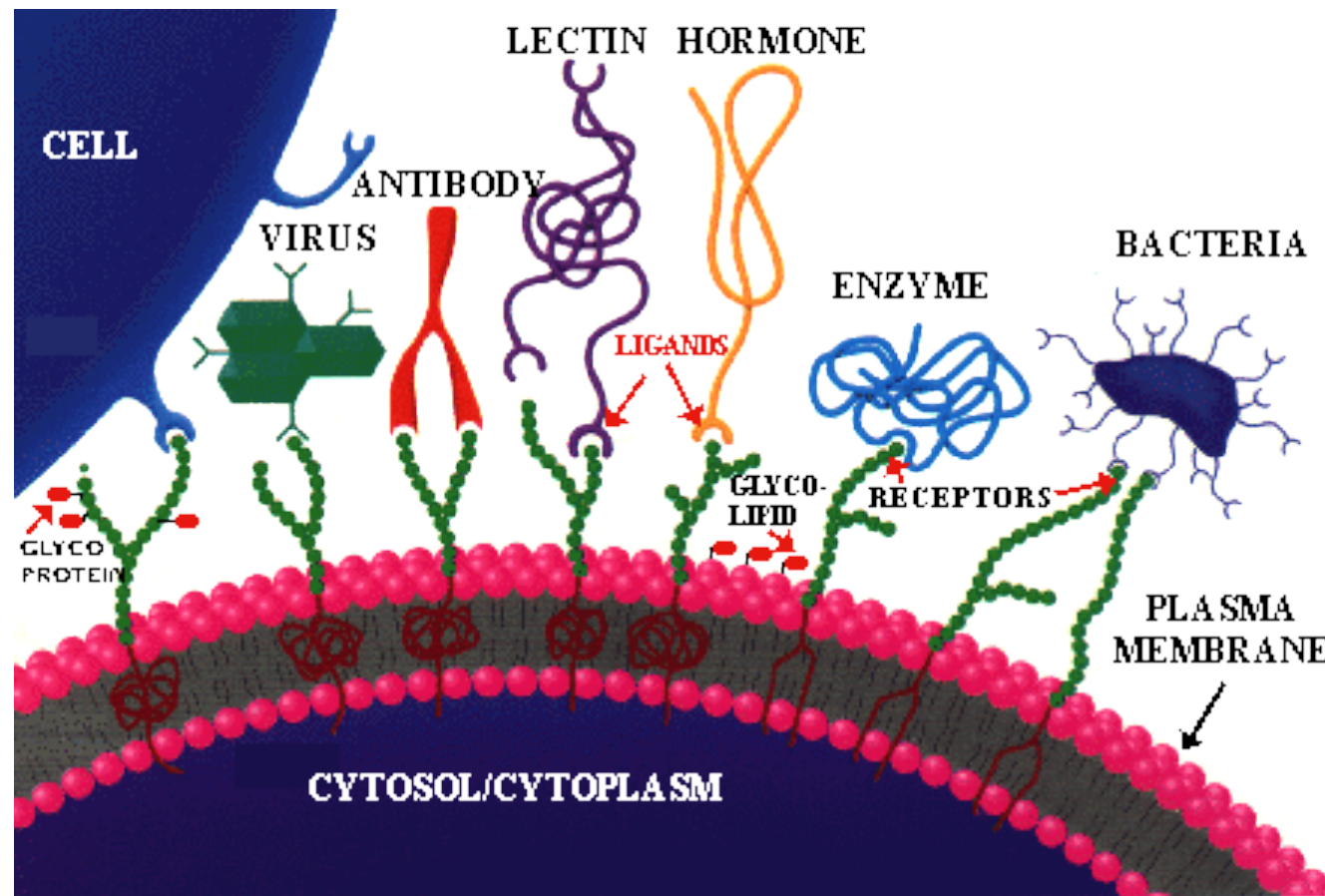


Surface Functionalization

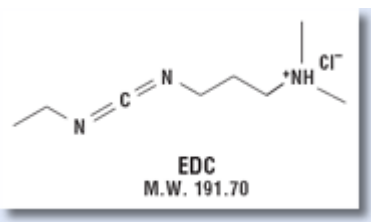
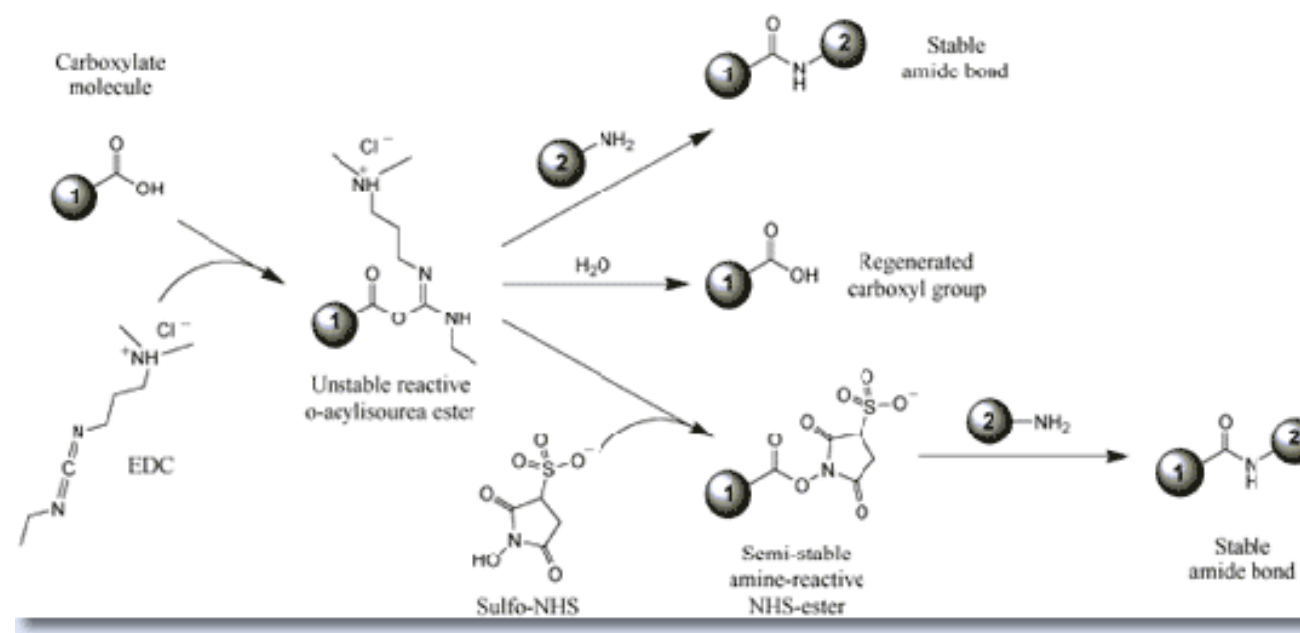
- Recognition
 - Molecular Recognition
 - Protein
 - DNA
 - Saccharide
- Reporting/Detection
 - Dye
 - Quantum dots
 - SPR
 - SERS/LSPR
- Separation
 - Gel/Chromatography
 - Magnetic
- Surfaces
 - Gold and silver
 - Silicon oxide (glass)
 - Quantum dots
 - Polymer



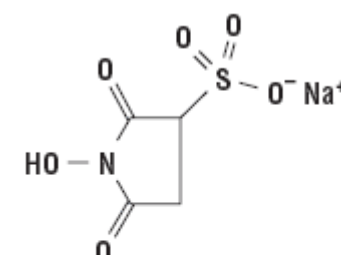
Molecular Recognition



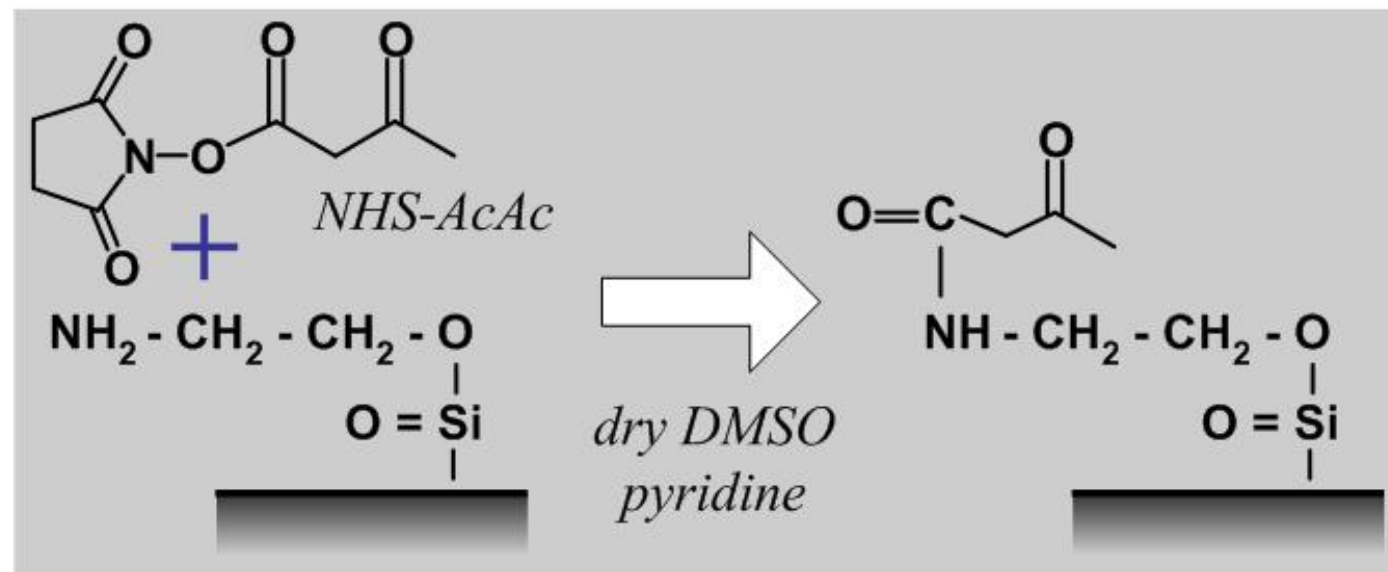
Carboxyl Presenting Surfaces



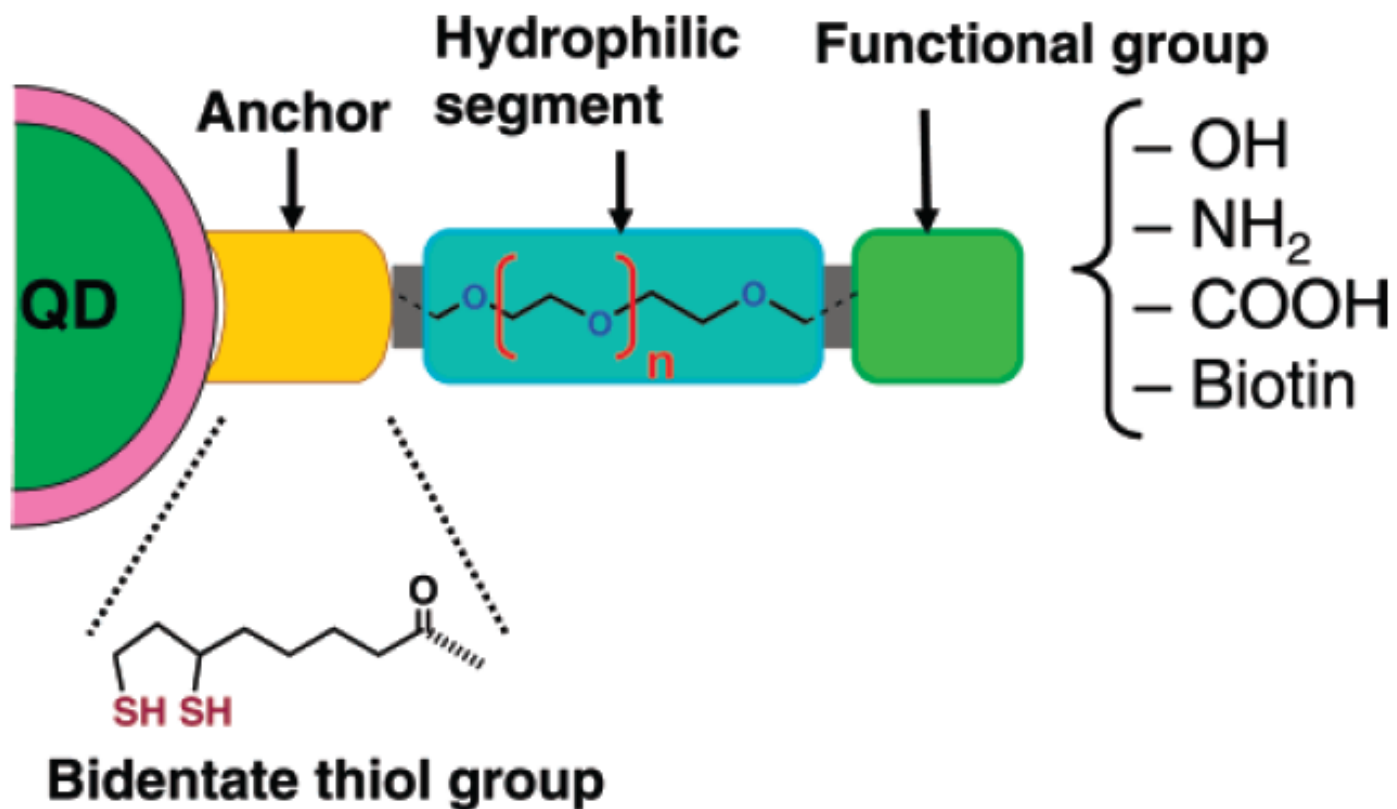
EDC (1-Ethyl-3-[3-dimethylaminopropyl]carbodiimide Hydrochloride)



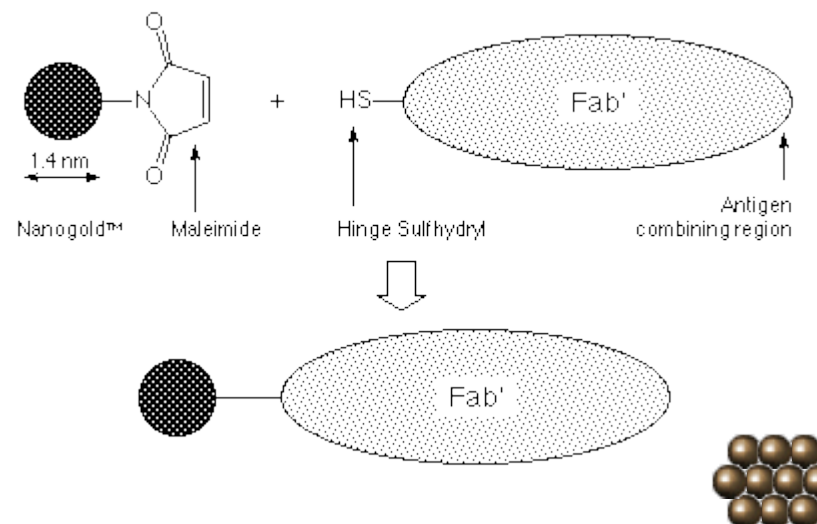
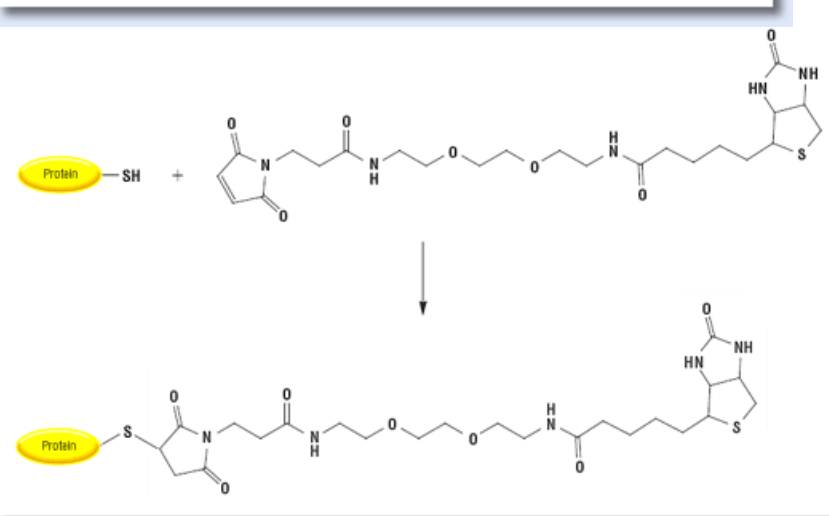
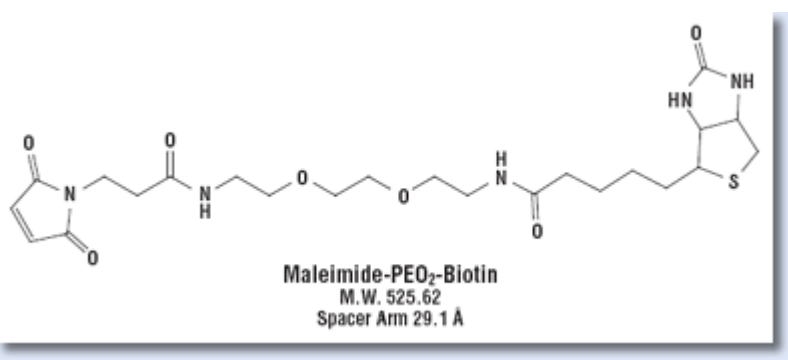
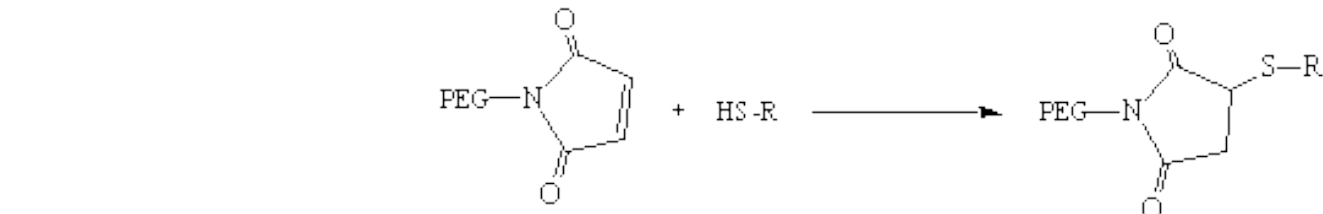
Amine Presenting Surface



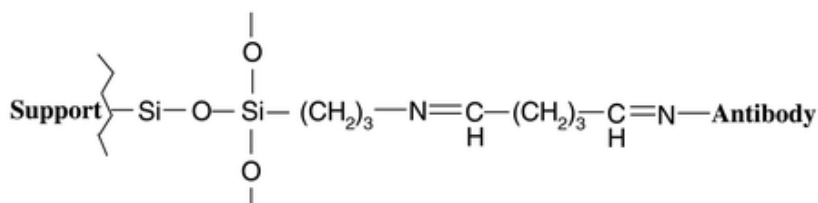
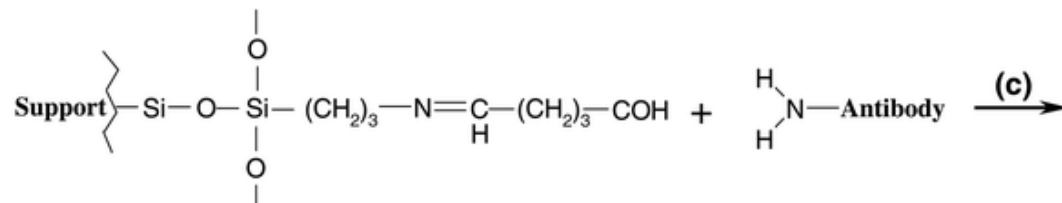
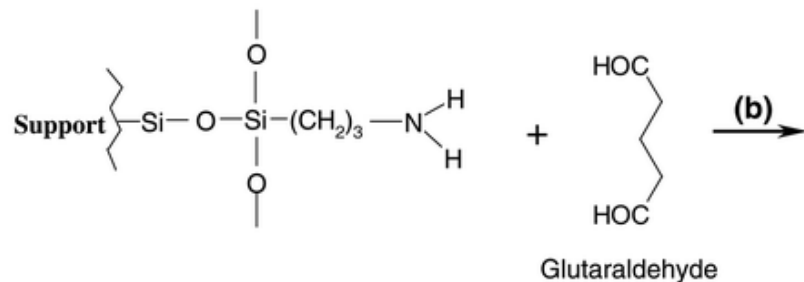
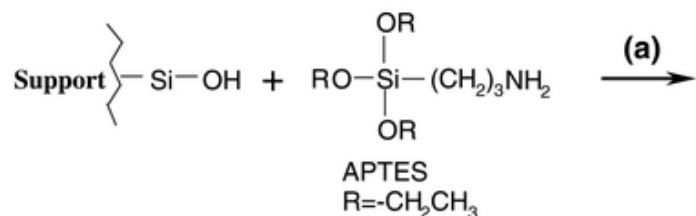
Scheme 1. Modular Design of Hydrophilic Ligands with Terminal Functional Groups Used in This Study



Sulfhydryl Labeling



Silica Modification



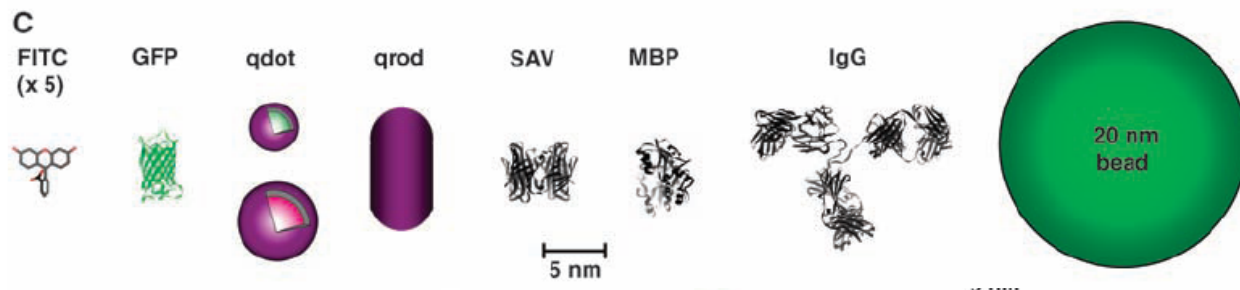
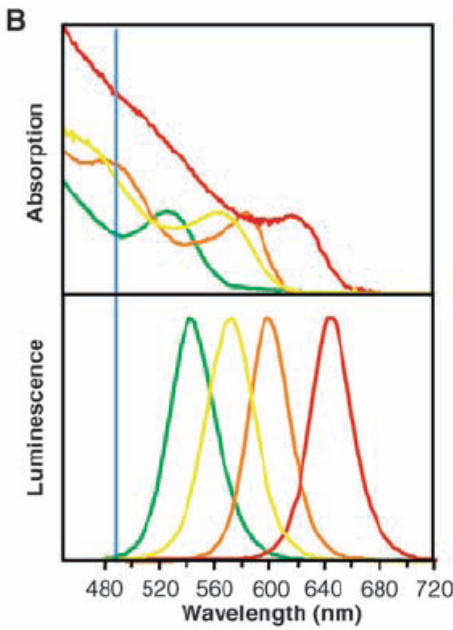
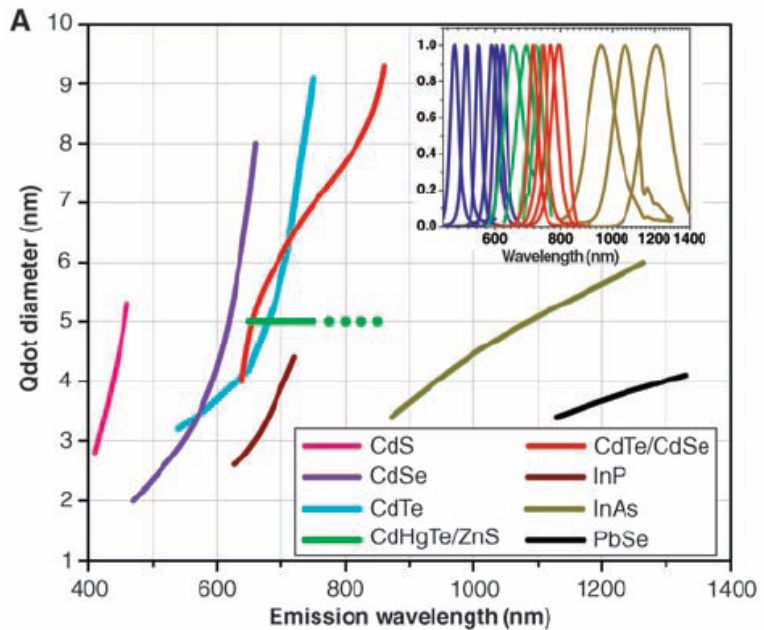
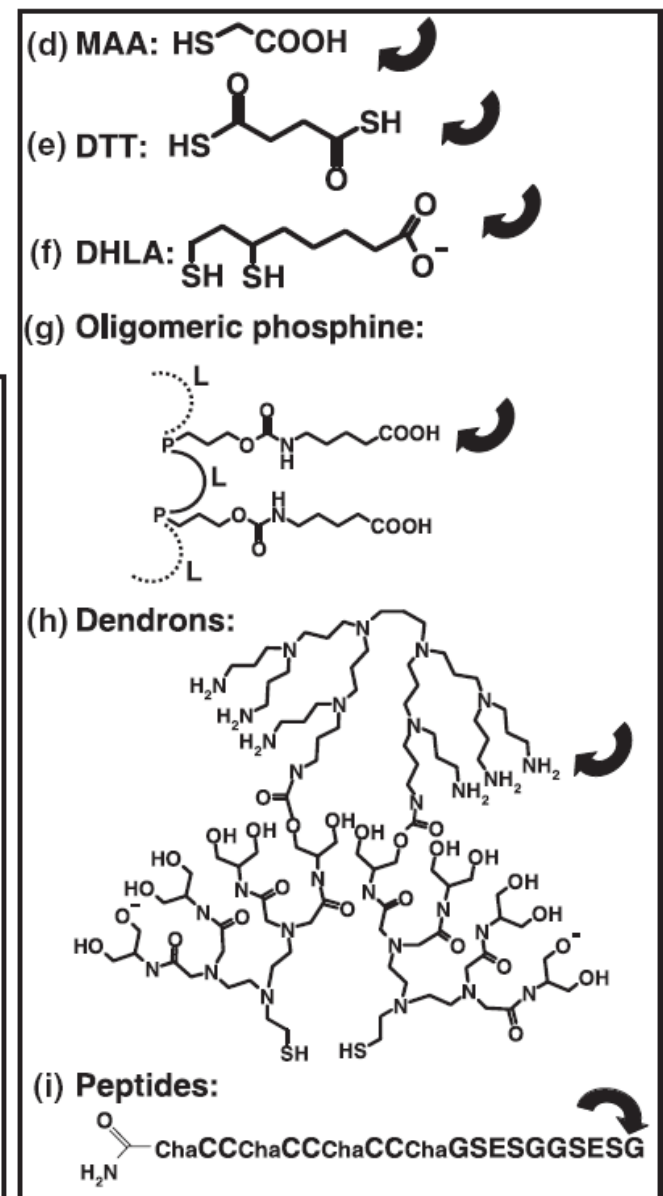
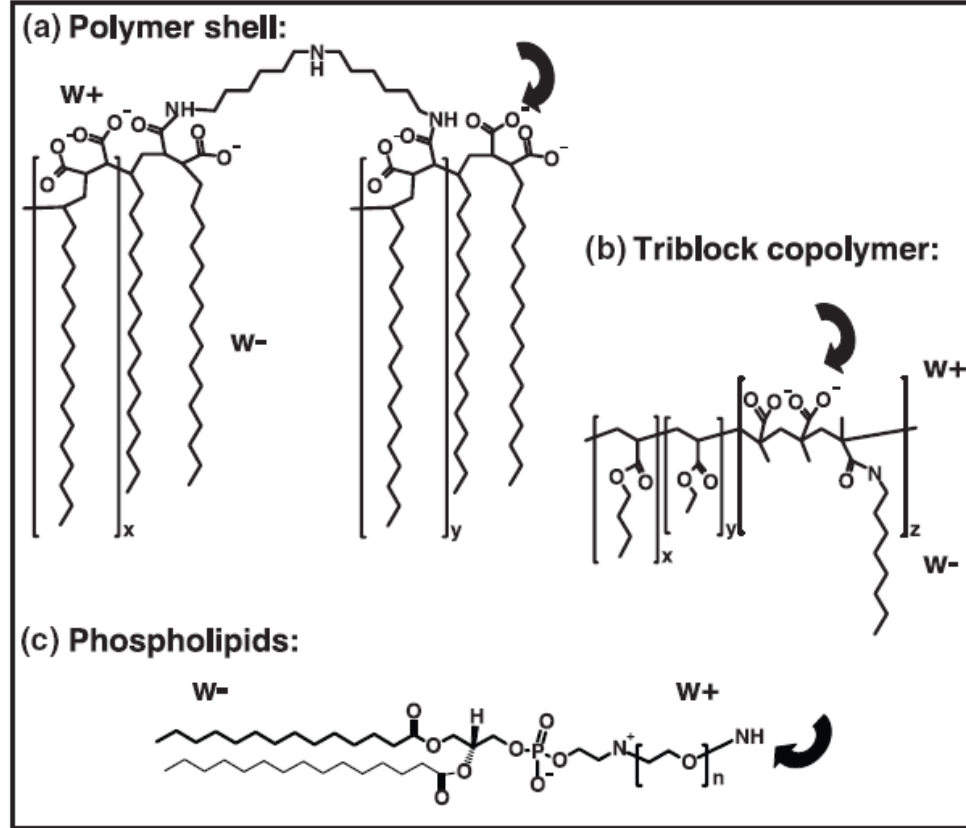
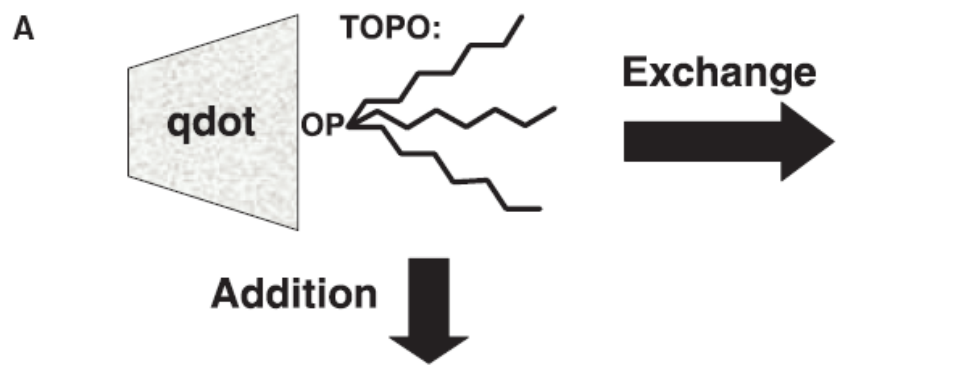
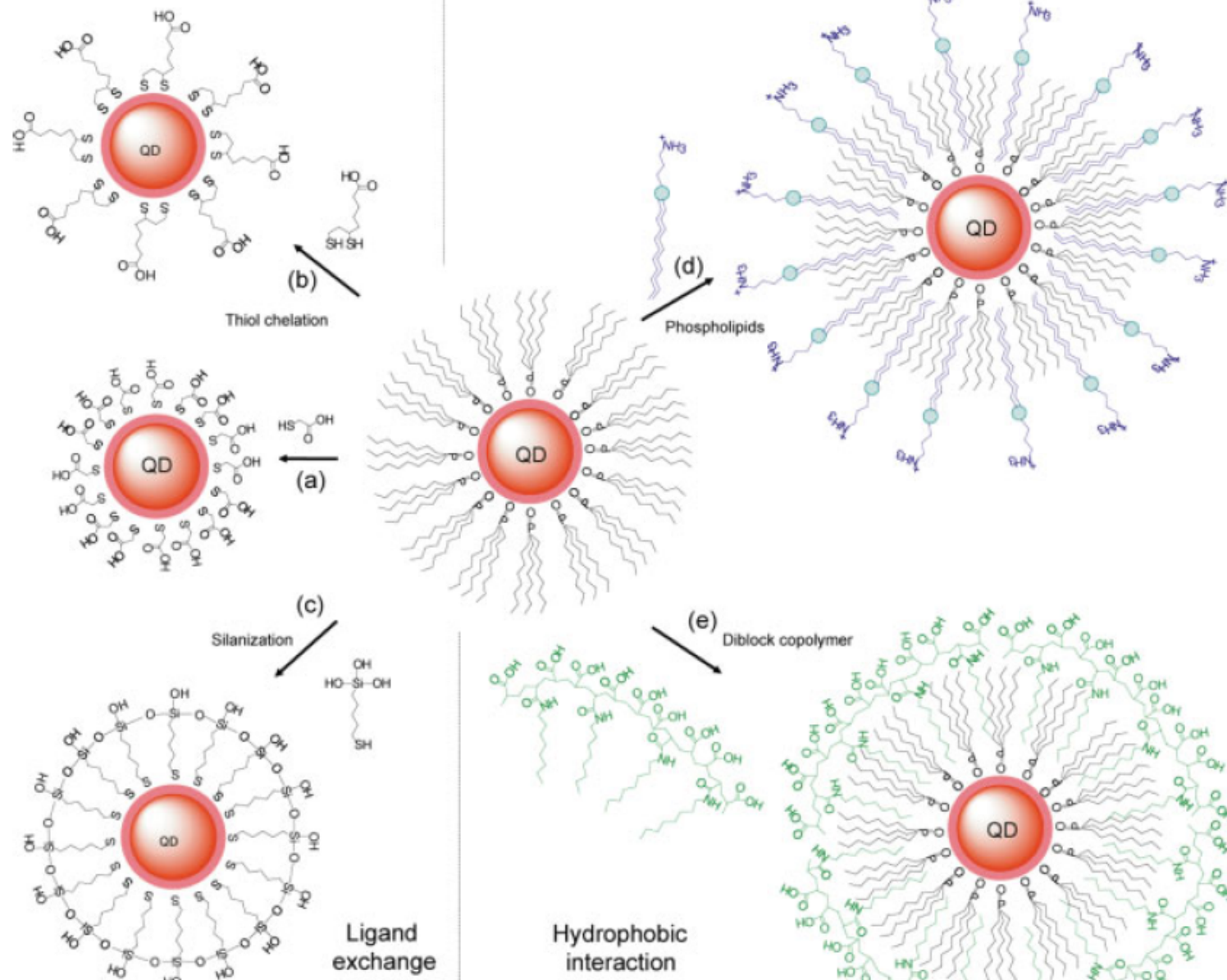


Fig. 1. (A) Emission maxima and sizes of quantum dots of different composition. Quantum dots can be synthesized from various types of semiconductor materials (II-VI: CdS, CdSe, CdTe...; III-V: InP, InAs...; IV-VI: PbSe...) characterized by different bulk band gap energies. The curves represent experimental data from the literature on the dependence of peak emission wavelength on qdot diameter. The range of emission wavelength is 400 to 1350 nm, with size varying from 2 to 9.5 nm (organic passivation/solubilization layer not included). All spectra are typically around 30 to 50 nm (full width at half maximum). Inset: Representative emission spectra for some materials. Data are from (12, 18, 27, 76–82). Data for CdHgTe/ZnS have been extrapolated to the maximum emission wavelength obtained in our group. (B) Absorption (upper curves) and emission (lower curves) spectra of four CdSe/ZnS qdot samples. The blue vertical line indicates the 488-nm line of an argon-ion laser, which can be used to efficiently excite all four types of qdots simultaneously. [Adapted from (28)] (C) Size comparison of qdots and comparable objects. FITC, fluorescein isothiocyanate; GFP, green fluorescent protein; qdot, green (4 nm, top) and red (6.5 nm, bottom) CdSe/ZnS qdot; qrod, rod-shaped qdot (size from Quantum Dot Corp.'s Web site). Three proteins—streptavidin (SAV), maltose binding protein (MBP), and immunoglobulin G (IgG)—have been used for further functionalization of qdots (see text) and add to the final size of the qdot, in conjunction with the solubilization chemistry (Fig. 2).







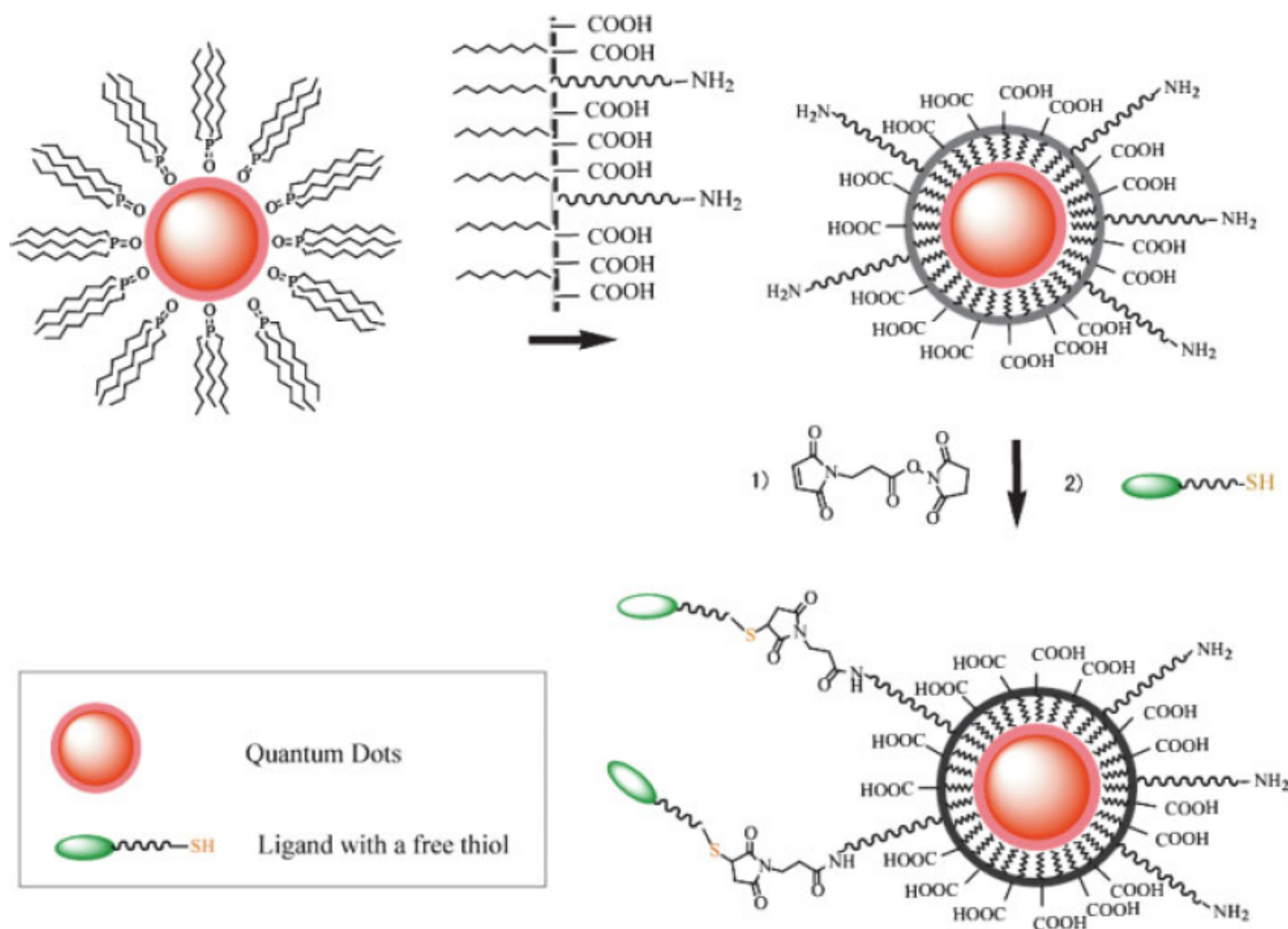
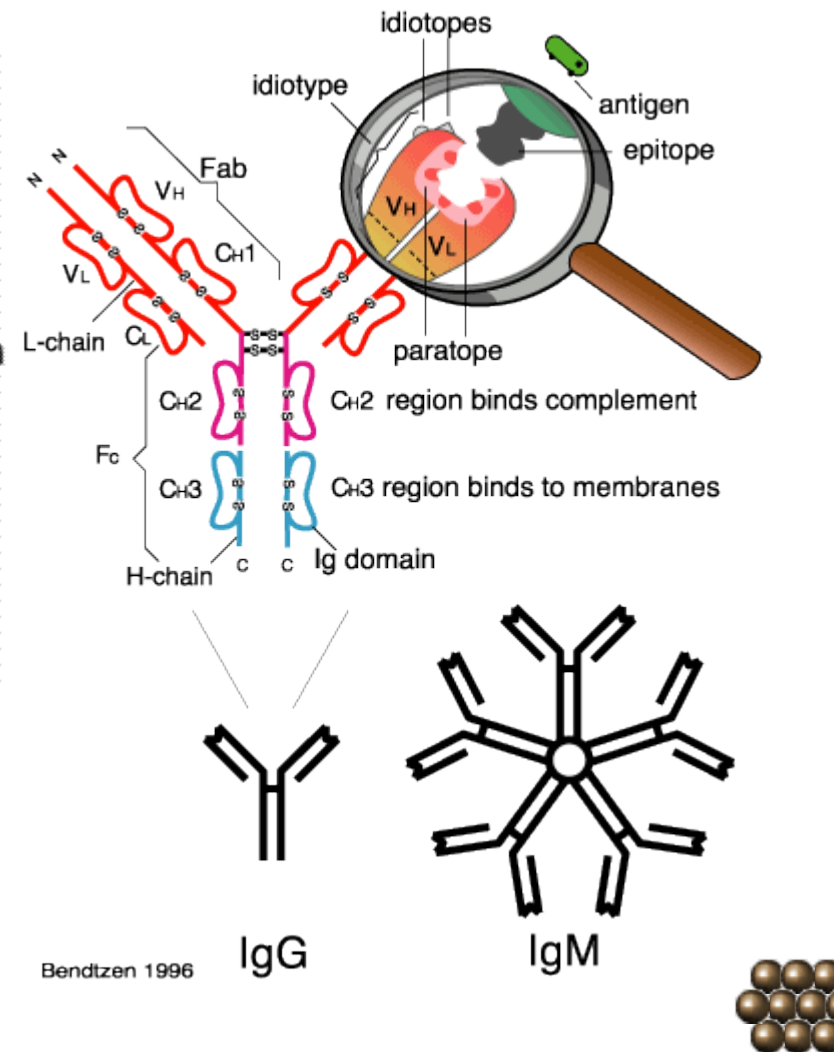
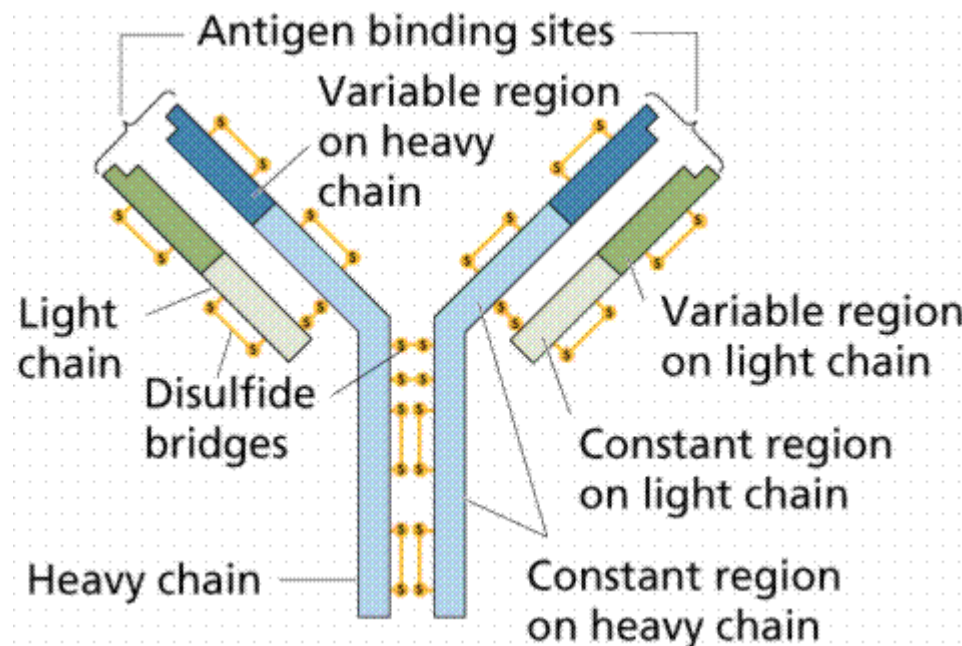


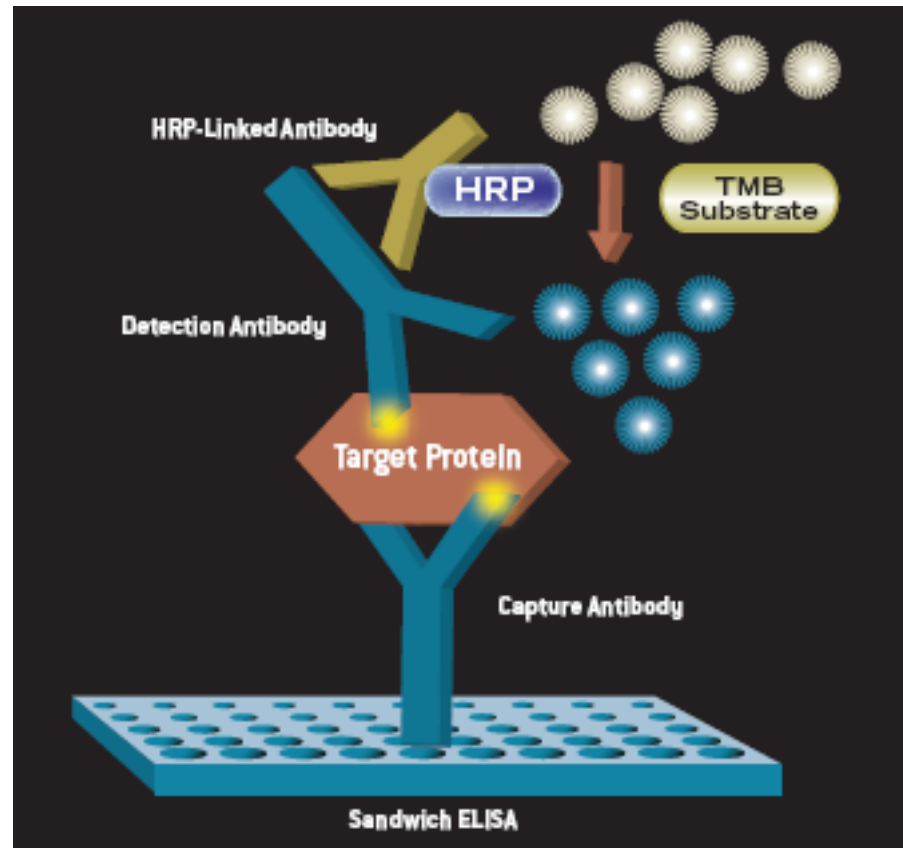
FIGURE 3 Maleimide functionalized QDs for conjugating thiol-containing ligands. TOPO stabilized QDs are coated with a primary amine functionalized tri-block amphiphilic copolymer for producing water-soluble QDs, which facilitate further conjugation to ligands with free thiols through bi-functional cross-linkers.



Antibody and Antigen



Enzyme-Linked ImmunoSorbent Assay (ELISA)

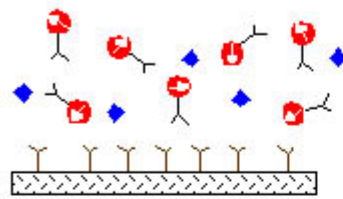


Labeling
BSA/PEG

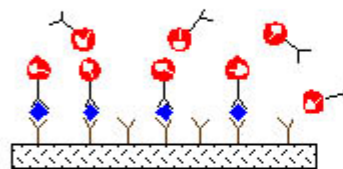


Microarray

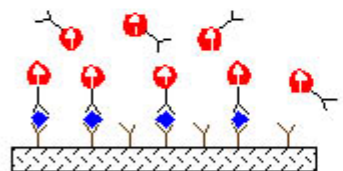
◆ Biomolecules of interest Y Capture antibody ■ Solid support ● Magnetically labeled antibody



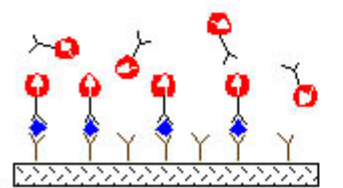
Add biomolecules of interest and magnetically labeled detect antibodies to well coated with capture antibody.



Immobilized immune complexes form on solid support.



Apply external magnetic field, magnetic dipoles align.

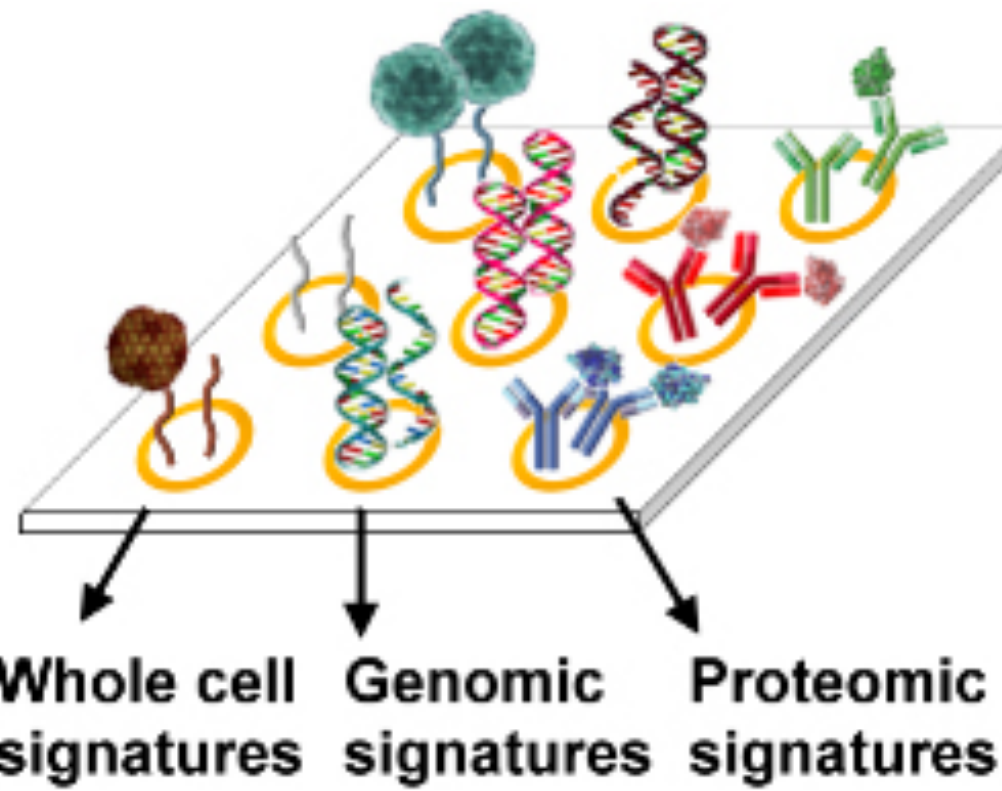


Remove field, measure net magnetization due to bound antibody labels. Unbound labels randomize quickly and contribute no net signal.

Detector



Microarray



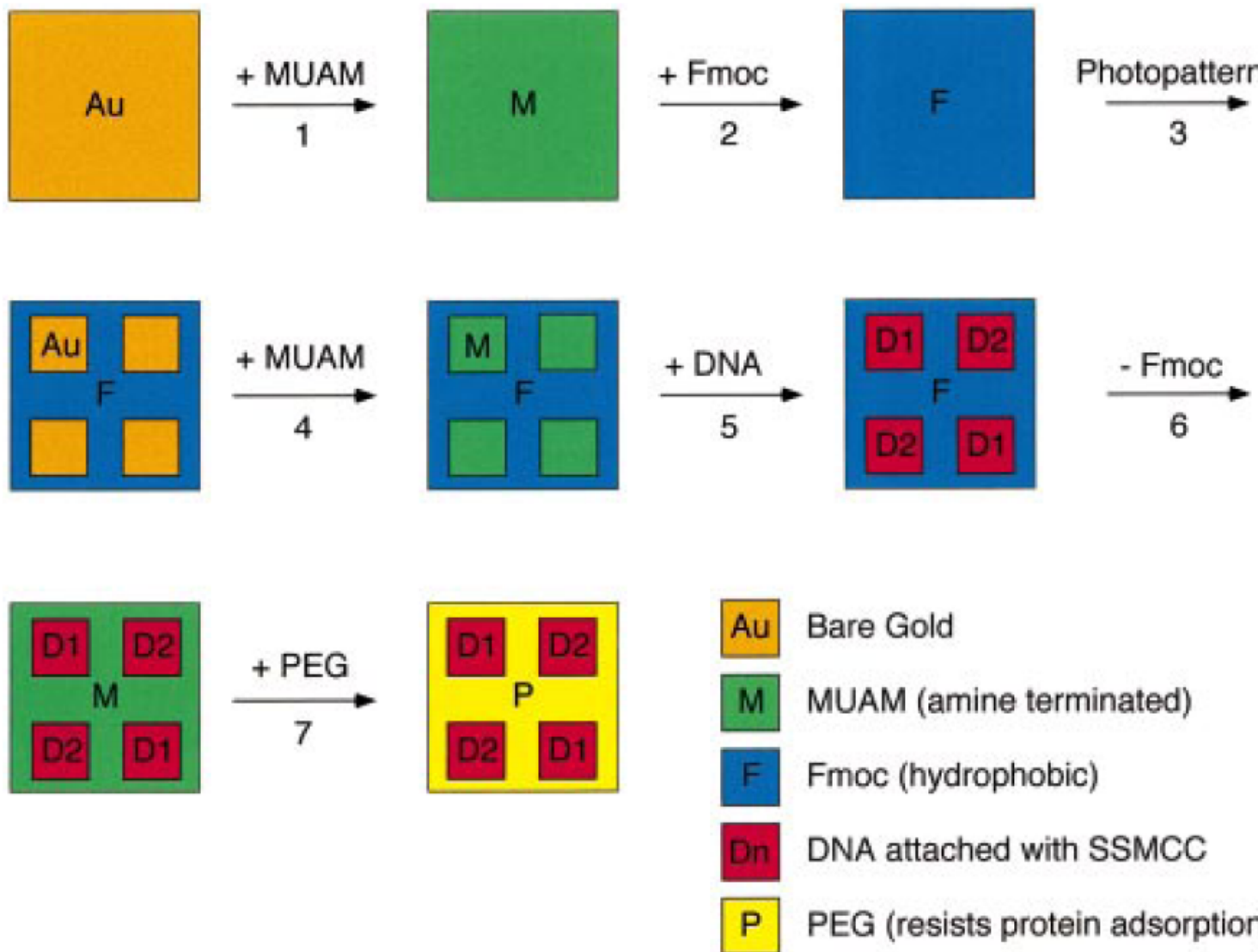


Figure 1. Fabrication scheme for the construction of multi-element DNA arrays. A clean gold surface is reacted with the amine-terminated alkanethiol MUAM, and subsequently reacted with Fmoc-NHS to create a hydrophobic surface. This surface is then exposed to UV radiation through a quartz mask and rinsed with solvent to remove the MUAM+Fmoc from specific areas of the surface, leaving bare gold pads. These bare gold areas on the sample surface are filled in with MUAM, resulting in an array of MUAM pads surrounded by a hydrophobic Fmoc background. Solutions of DNA are then delivered by pipet onto the specific array locations and are covalently bound to the surface via the bifunctional linker SSMCC. In the final two steps, the Fmoc-terminal groups on the array background are removed and replaced by PEG groups which prohibit the nonspecific binding of analyte proteins to the background.



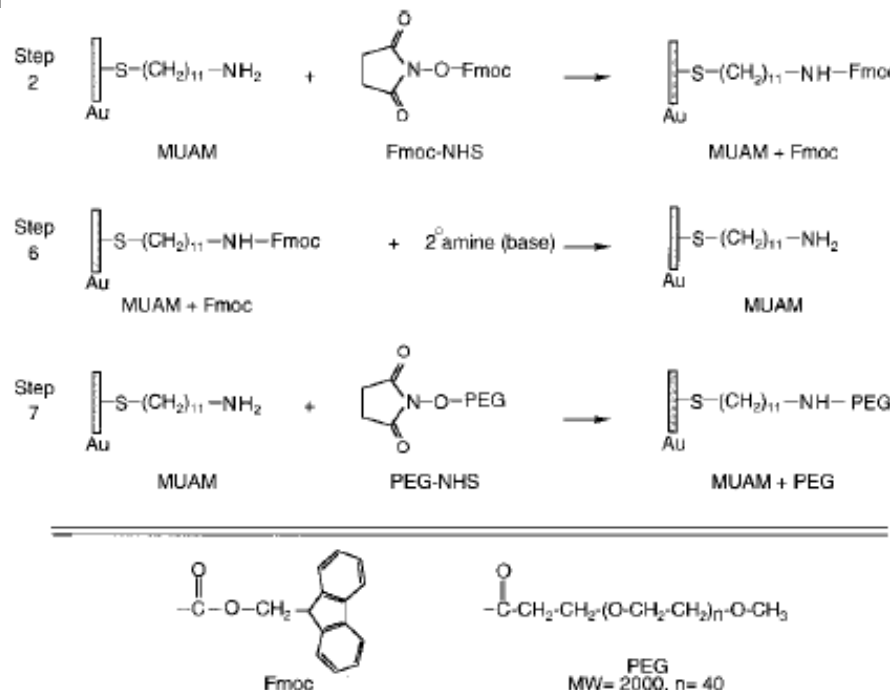


Figure 2. Surface reaction scheme showing the steps involved in the reversible modification of the array background. (Step 2) The starting amine-terminated alkanethiol surface (MUAM) is reacted with the Fmoc-NHS protecting group to form a carbamate linkage thus creating a hydrophobic Fmoc-terminated surface. (Step 6) After DNA immobilization (see Figure 3), the hydrophobic Fmoc group is removed from the surface with a basic secondary amine, resulting in the return of the original MUAM surface. (Step 7) In the final array fabrication step, the deprotected MUAM is reacted with PEG-NHS to form an amide bond that covalently attaches PEG to the array surface.

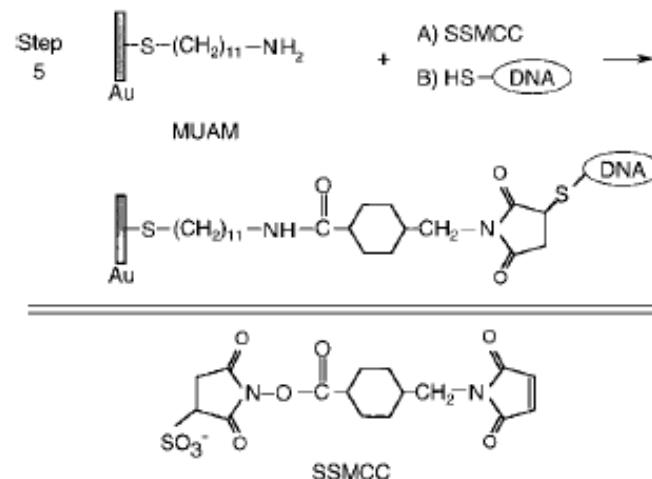
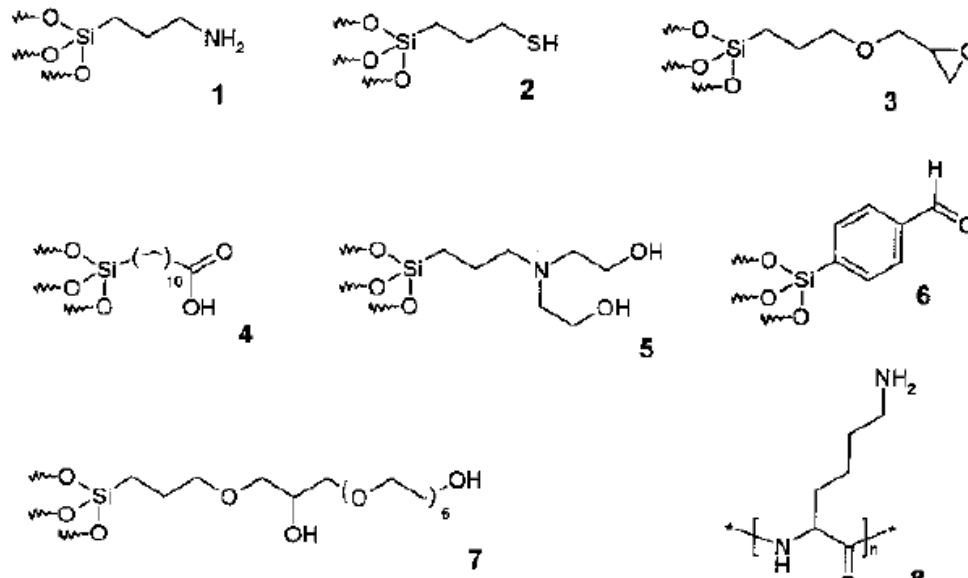
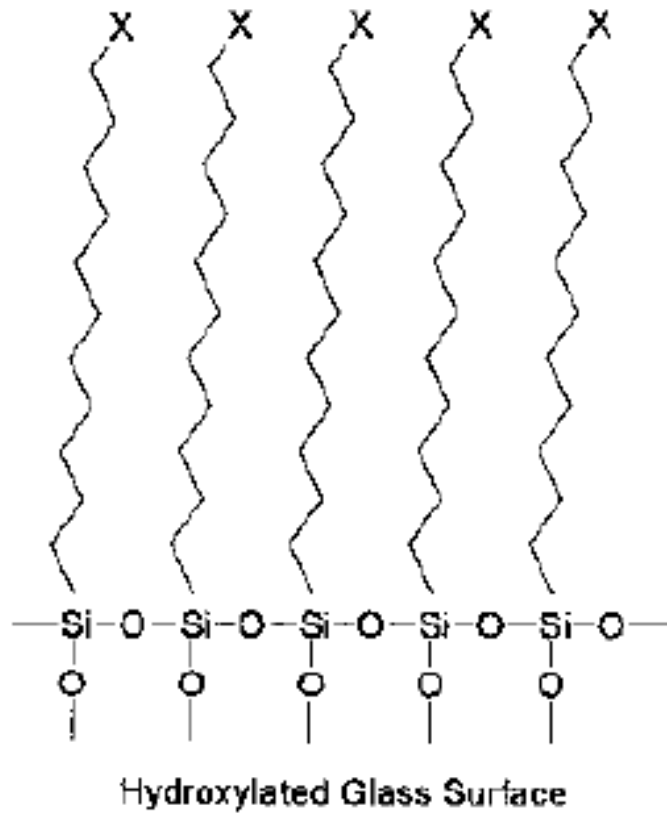


Figure 3. Surface reaction scheme showing the immobilization of thiol-terminated DNA to the array surface. In Step 5 of the DNA array fabrication, the heterobifunctional linker SSMCC is used to attach 5'-thiol modified oligonucleotide sequences to reactive pads of MUAM. This linker contains an NHSS ester functionality (reactive toward amines) and a maleimide functionality (reactive toward thiols). The surface is first exposed to a solution of the linker, whereby the NHSS ester end of the molecule reacts with the MUAM surface. Excess linker is rinsed away and the array surface is then spotted with 5'-thiol-modified DNA that reacts with the maleimide groups forming a covalent bond to the surface monolayer.

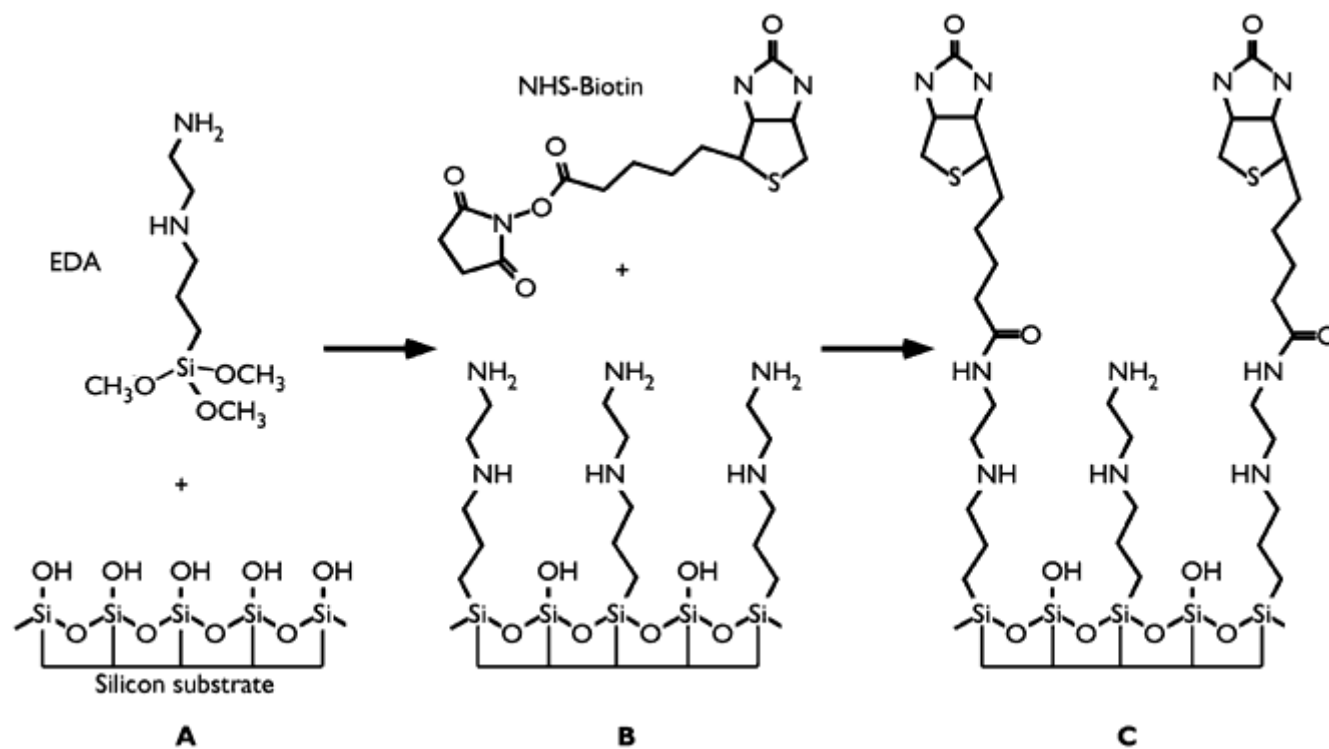


Glass Surface Modification



Scheme 2.2 Reagents for derivatization of glass surfaces. 1 APTES = aminopropyltriethoxysilane; 2 MPTS = 3-mercaptopropyltrimethoxysilane; 3 GPTS = glycidoxypropyltrimethoxysilane; 4 TETU = triethoxysilane undecanoic acid;

Scheme 2.1 2D schematic description of a polysiloxane monolayer on a glass surface (X = terminal functional)



Biotin-Streptavidin

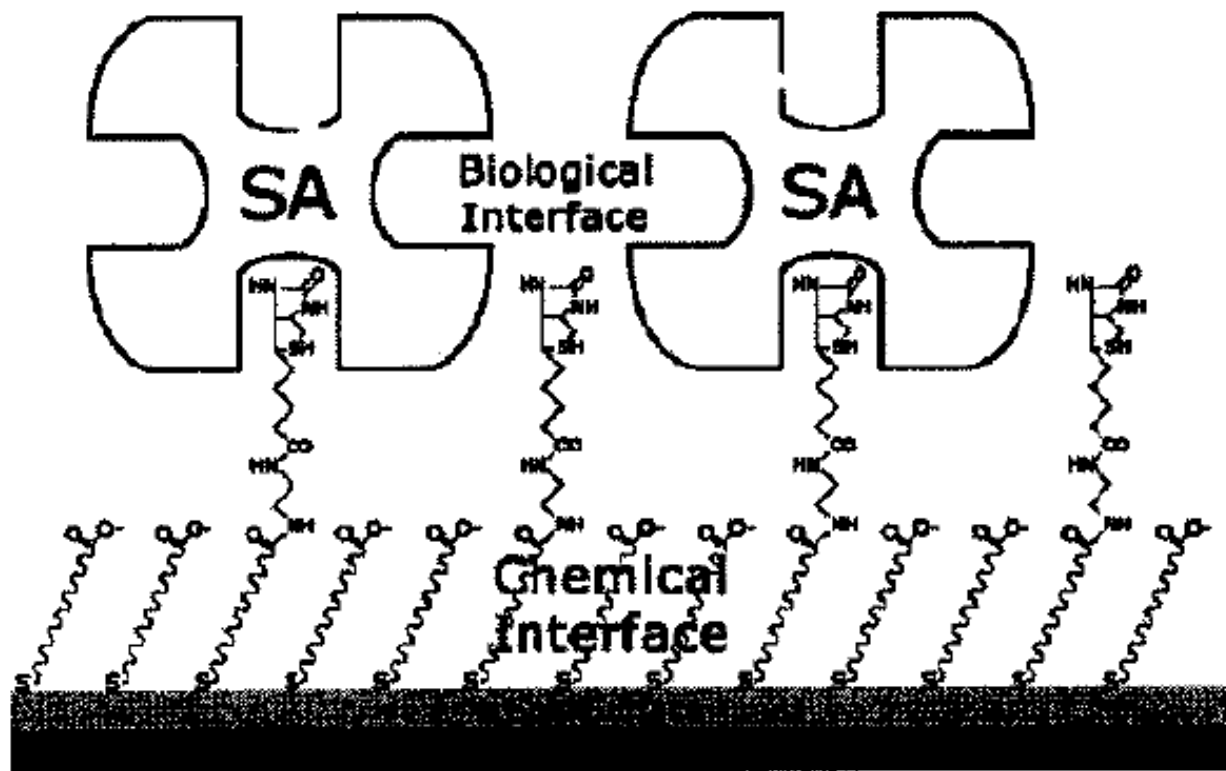
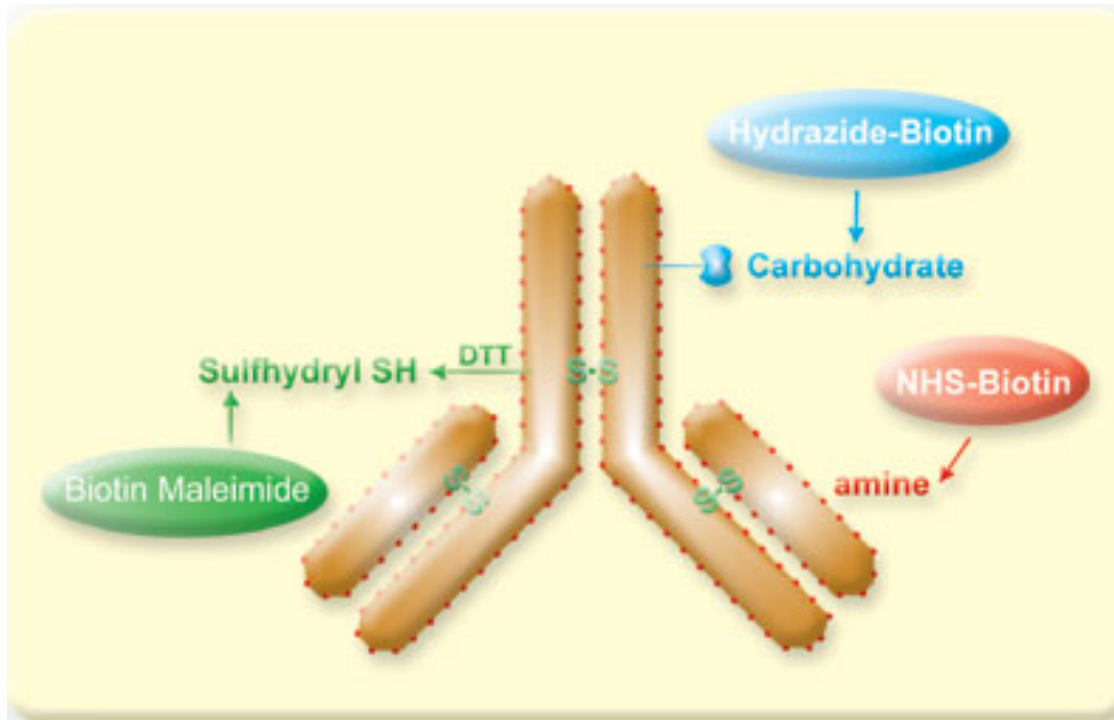


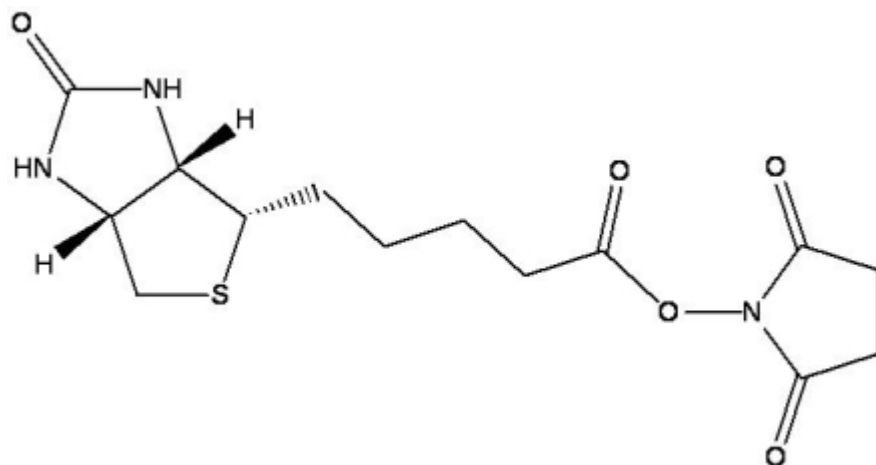
Figure 2.3 Schematic representation of a streptavidin sensor surface assembled on a reaction-controlled biotinylated SAM [28].



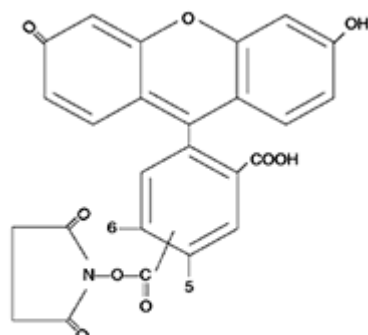
Protein Labeling



Amine Reactive Labeling



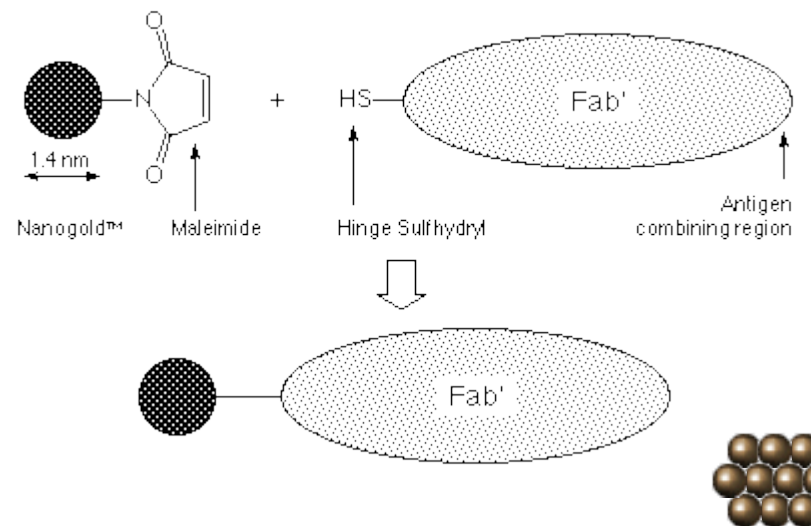
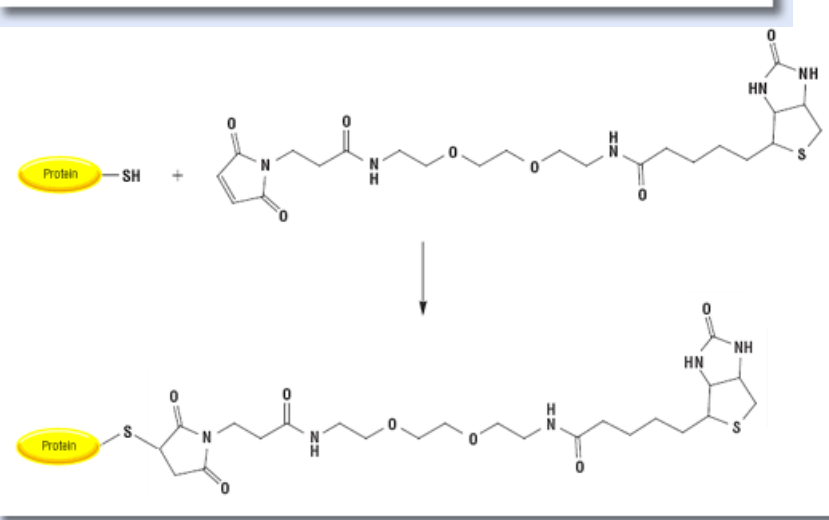
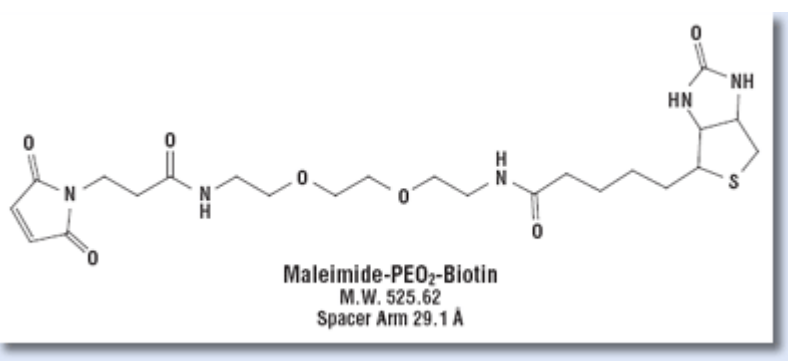
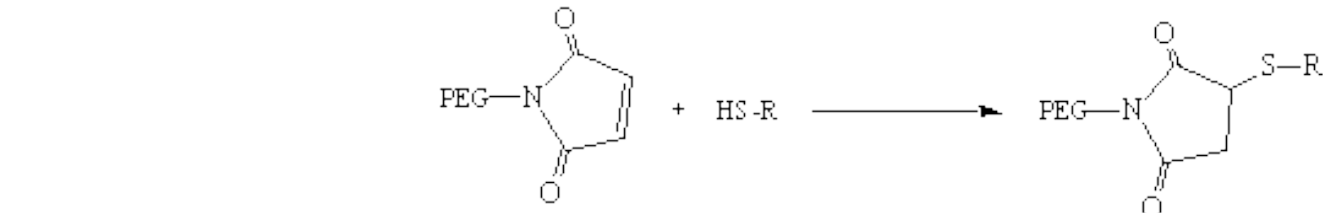
NHS ester

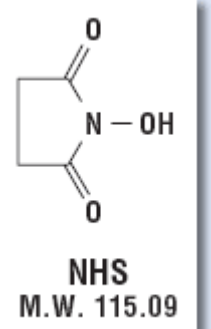
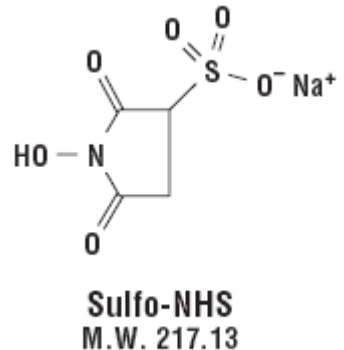


NHS-Fluorescein
MW 473.4



Sulfhydryl Labeling

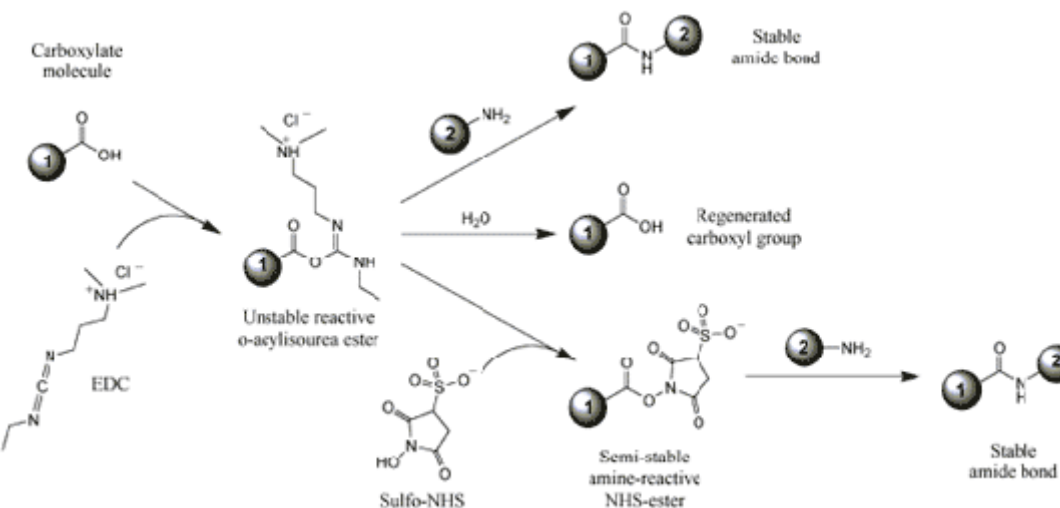
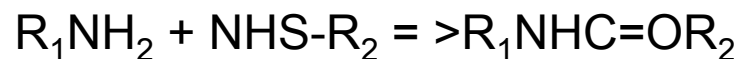




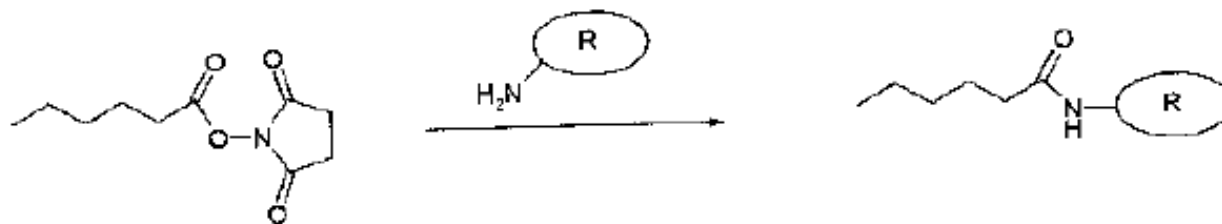
The most popular NH₂- and SH- crosslinker

N-hydroxysuccinimide

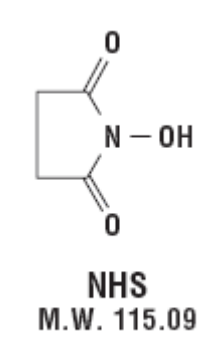
NH₂ => amide



N-hydroxysuccinimide (NHS)



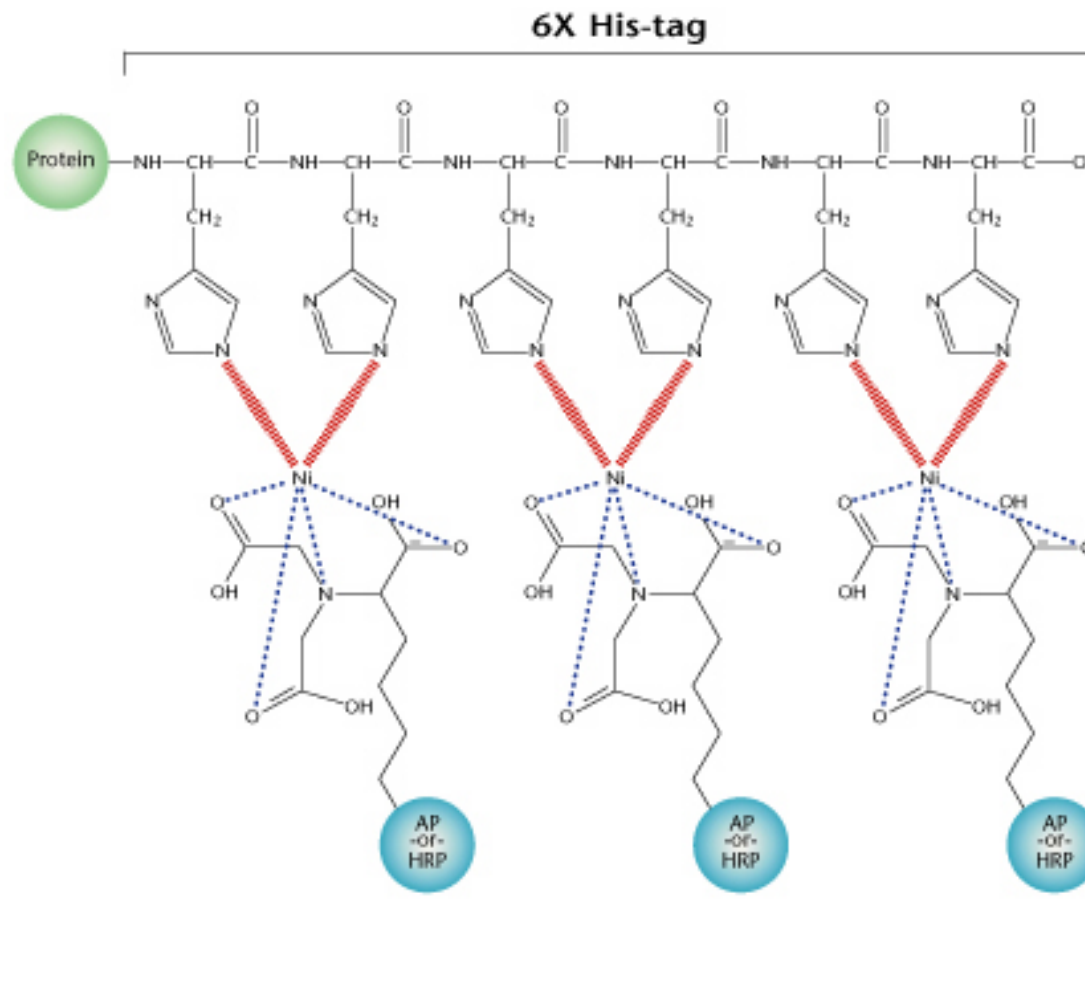
Scheme 2.6 Surface coupling reaction of NHS-esters with the amino residues of the side-chains of polypeptides (lysine units). R, protein.



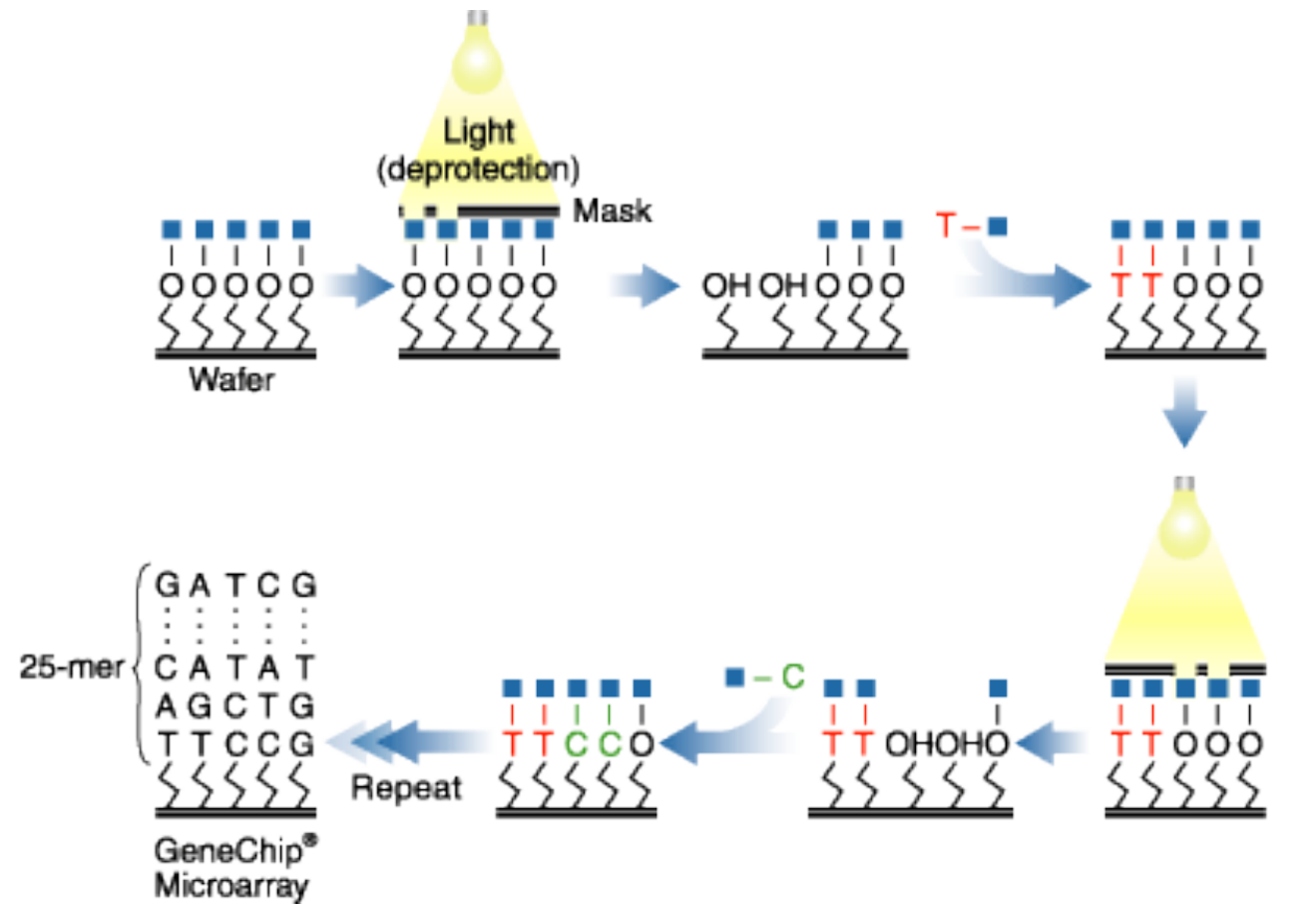
N-hydroxysuccinimide



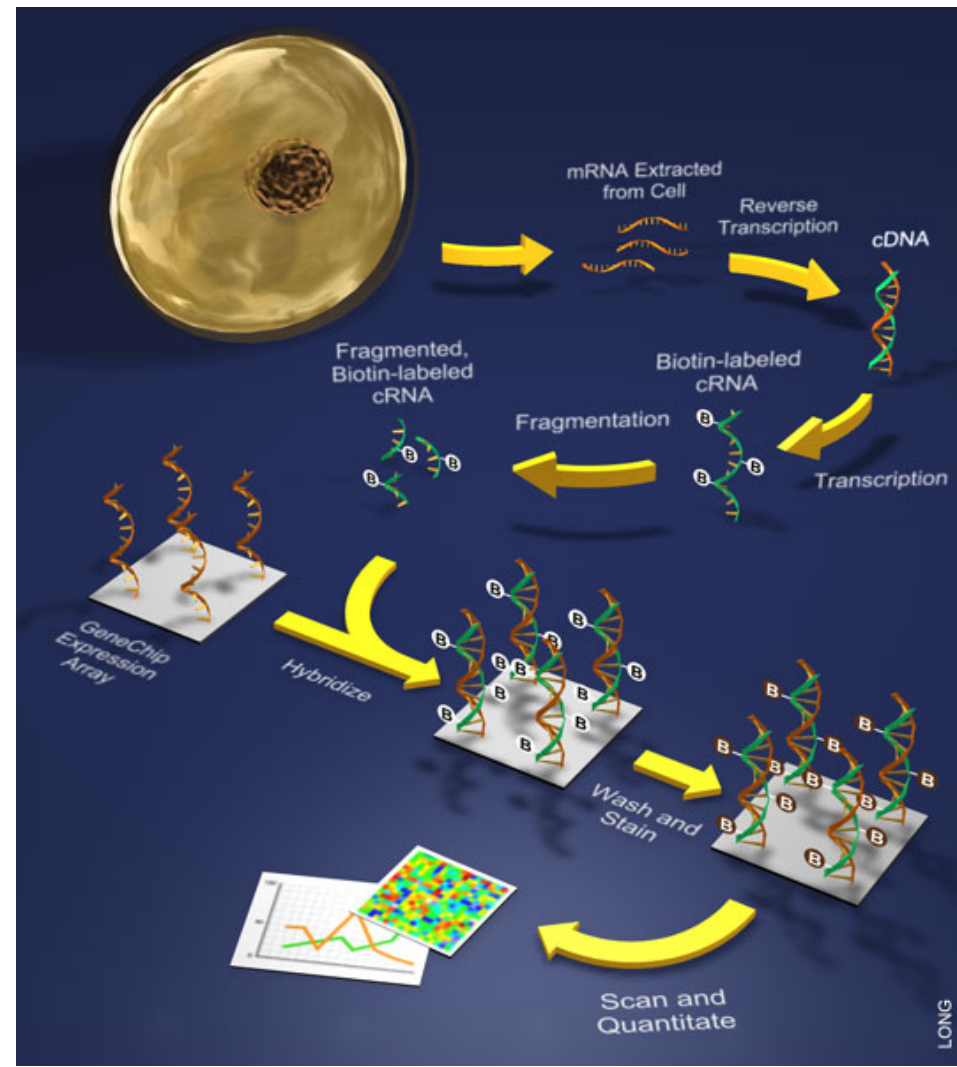
His Tag



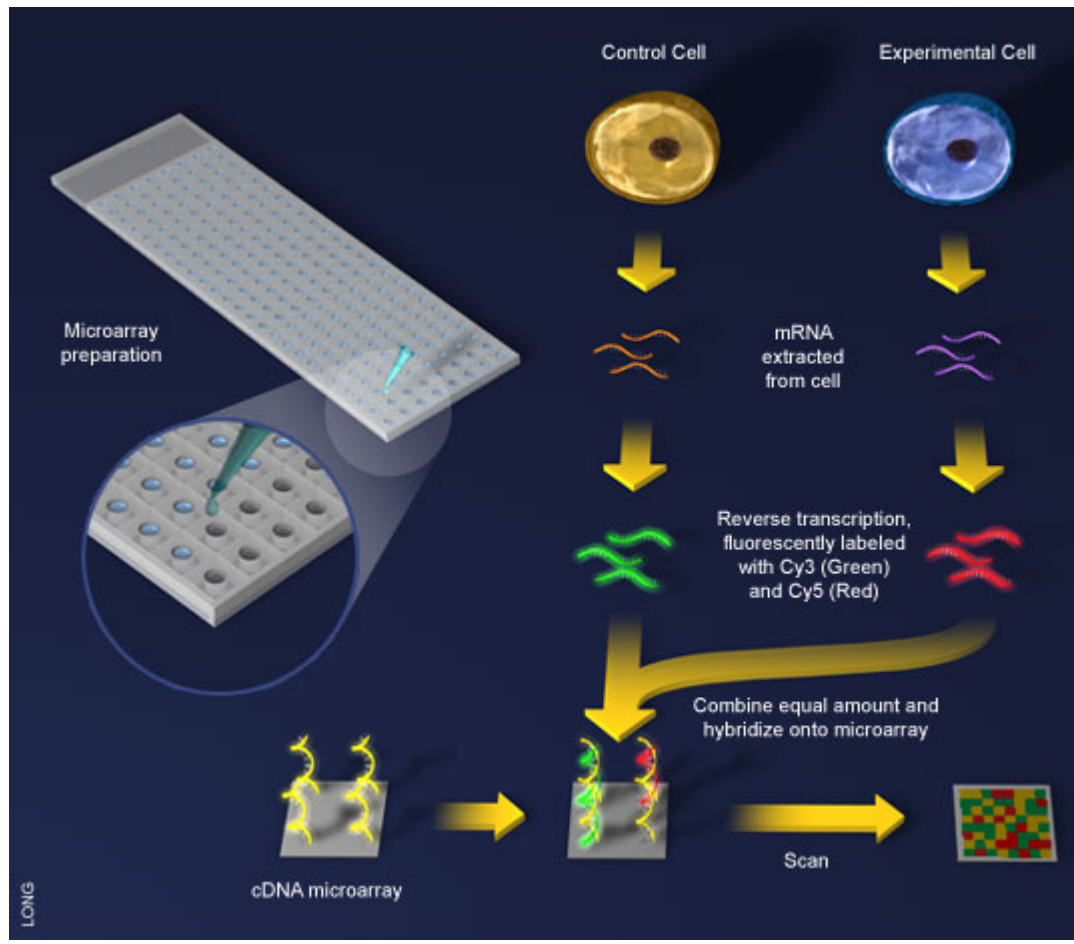
GeneChip



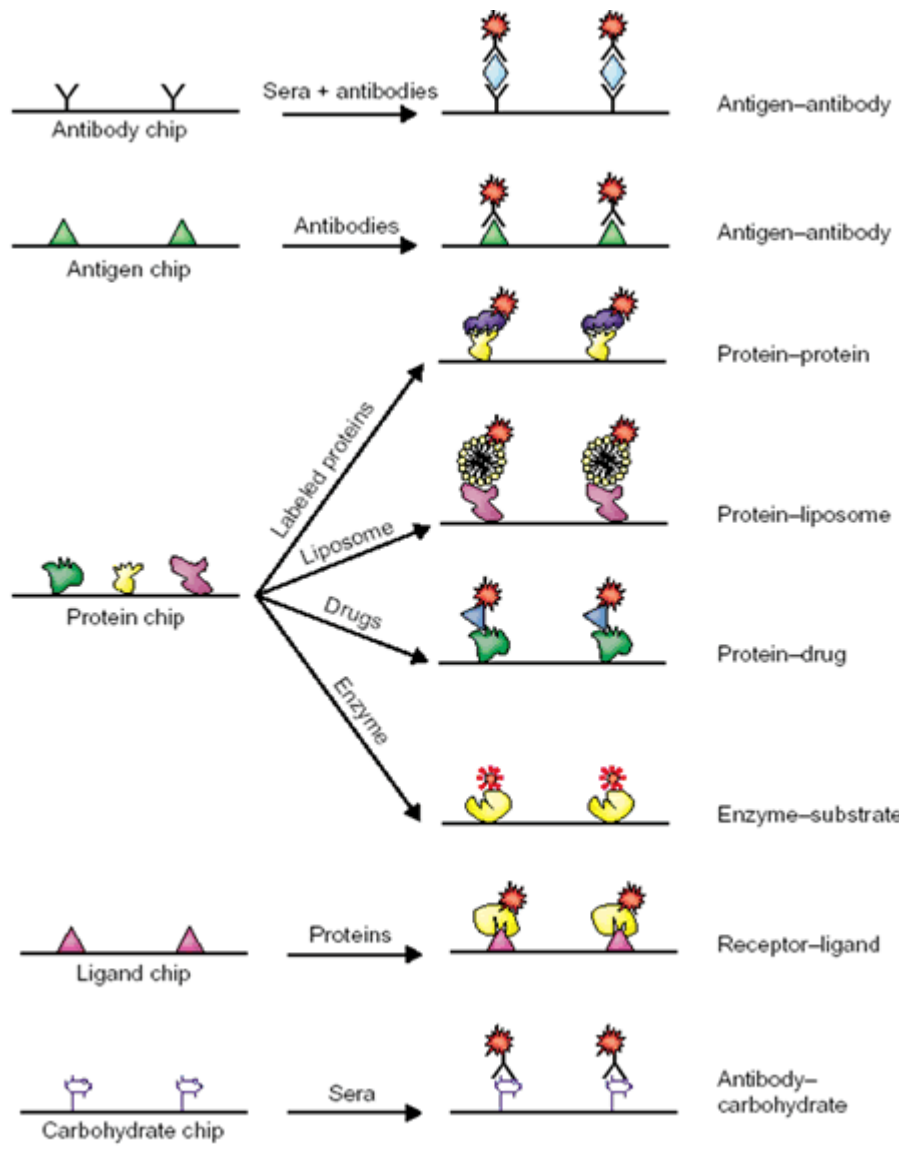
Scheme



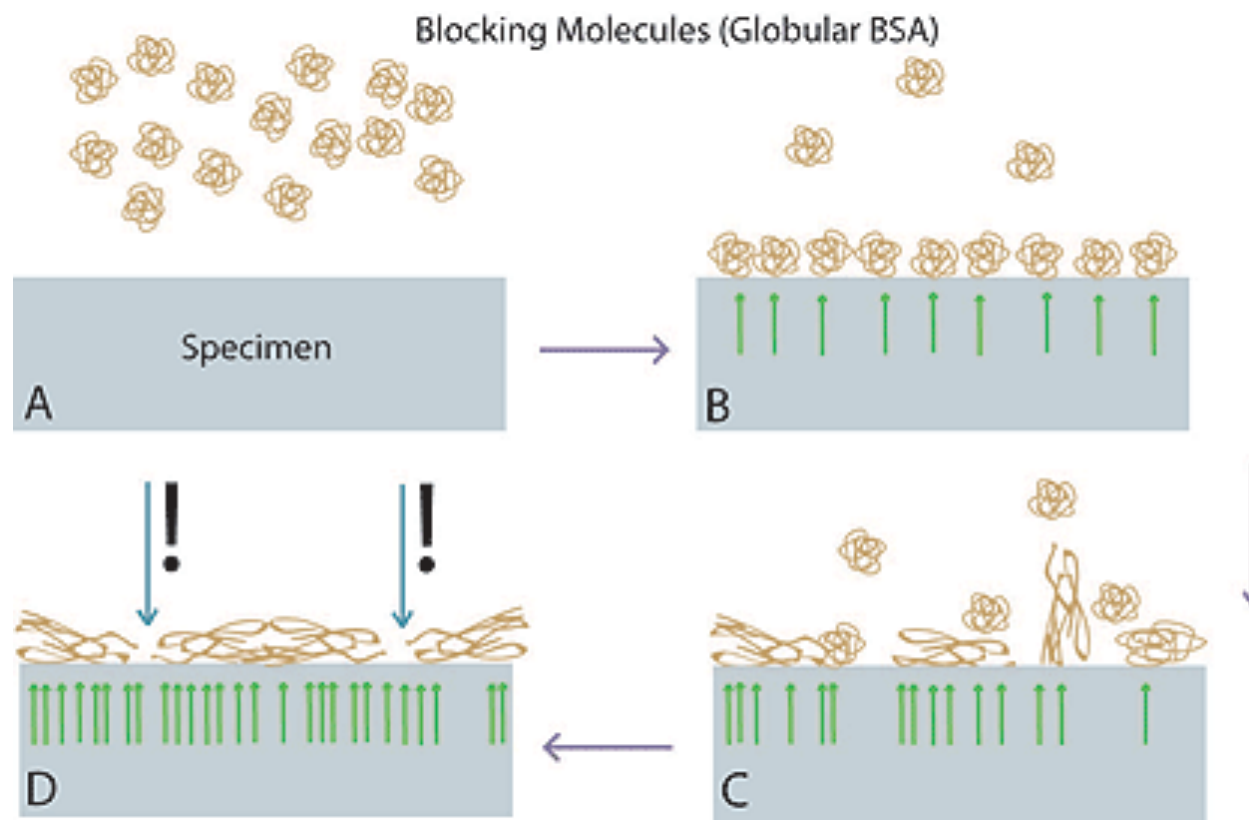
cDNA Microarray



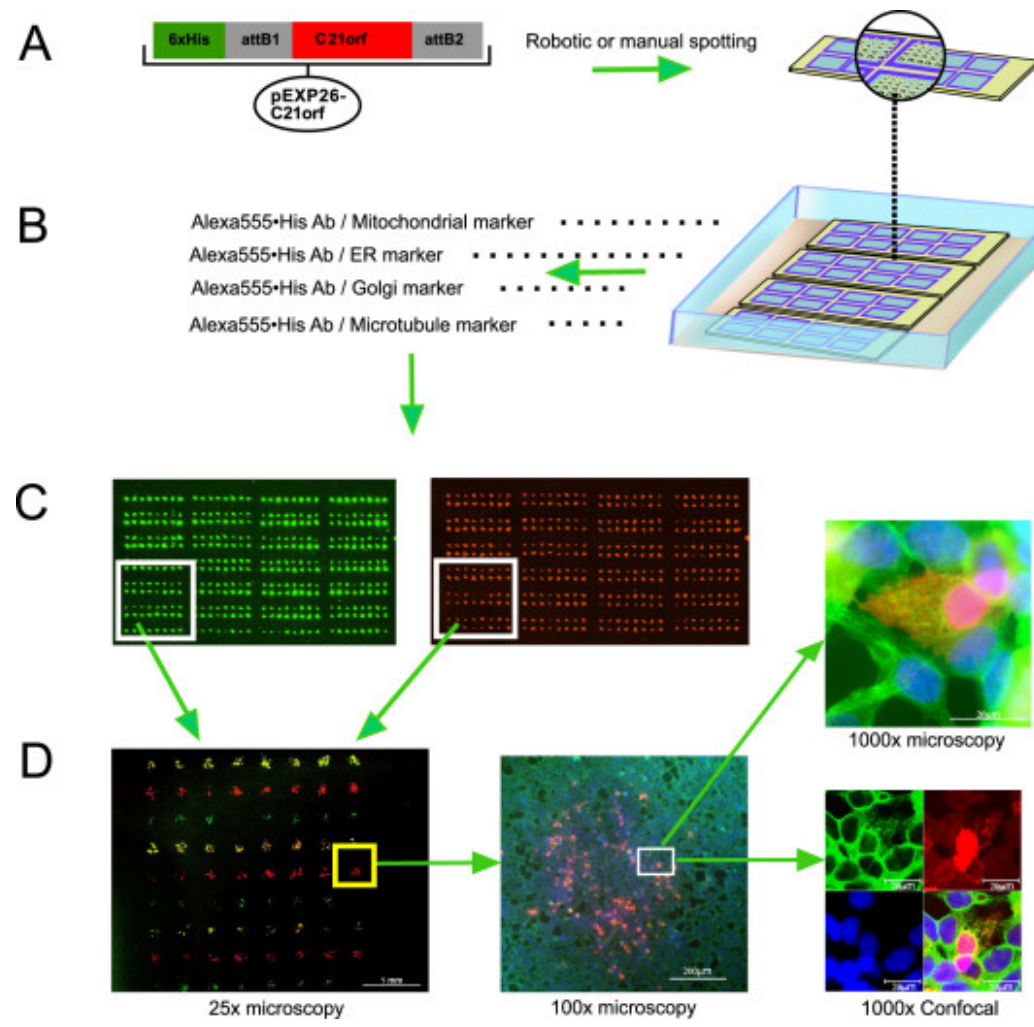
Protein Array



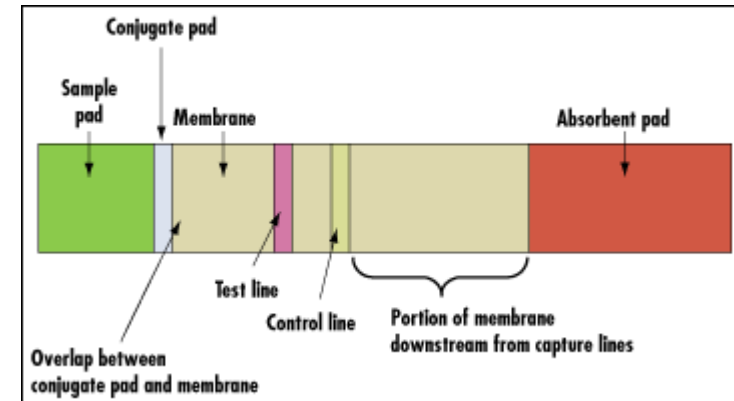
BSA Blocking



Cell Array



hCG immunoassay



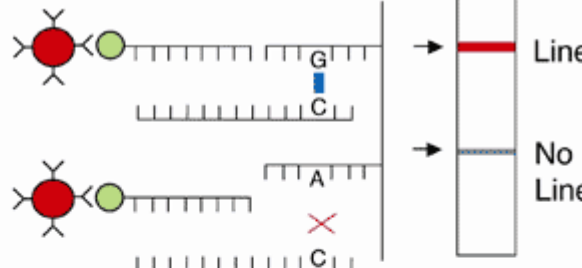
human chorionic gonadotropin (hCG)



Nucleotide Sensor

A)

Fully complementary

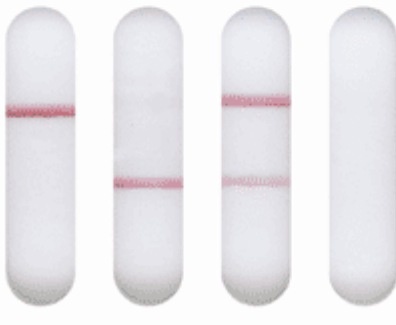


Line

No Line

Single mismatch

B)



- ← Capture probe G
- ← Capture probe A

Target nucleotide

